Published OnlineFirst February 4, 2013; DOI: 10.1158/0008-5472.CAN-12-3479

Combined treatment with vorinostat with gefitinib shrinks tumors produced by *EGFR*-mutant NSCLC cells with the *BIM* polymorphism

We next determined the *in vivo* efficacy of vorinostat and gefitinib. Gefitinib alone almost completely shrunk xenograft tumors induced by HCC827 cells (Fig. 3A). Although gefitinib monotherapy prevented the enlargement of tumors produced by PC-3 cells, which harbor the *BIM* polymorphism, it did not induce their complete regression, indicating that PC-3 cells remained less susceptible to gefitinib *in vivo*. Under these experimental conditions, vorinostat monotherapy inhibited tumor growth slightly, whereas the combination of vorinostat with gefitinib resulted in marked tumor shrinkage (Fig. 3B). None of the mice treated with these agents showed any macroscopic adverse effects, including loss of body weight (data not shown).

To clarify the mechanisms by which vorinostat and gefitinib act *in vivo*, we assessed tumor-cell apoptosis by TUNEL staining. Gefitinib treatment increased the number of apoptotic cells in HCC827 tumors but had little effect on PC-3 tumors (Fig. 4A and B), indicating that *EGFR*-mutant NSCLC cells with the *BIM* polymorphism are refractory to gefitinib-induced apoptosis *in vivo* as well as *in vitro*. Importantly, although vorinostat alone had little effect on apoptosis, the combination of vorinostat and gefitinib induced marked apoptosis in PC-3 tumors (Fig. 4A and B). Western blot analyses showed that gefitinib induced cleavage of caspase-3 in HCC827, but not in PC-3, tumors. In PC-3 tumors, treatment with gefitinib or vorinostat had little effect on caspase-3 cleavage, whereas their combination increased BIM expression and the cleavage of caspase-3 (Fig. 4C and D). These findings indicate that the combination of vorinostat and gefitinib increases BIM protein expression and induces tumor-cell apoptosis, thereby shrinking tumors produced by *EGFR*-mutant NSCLC cells with the *BIM* polymorphism.

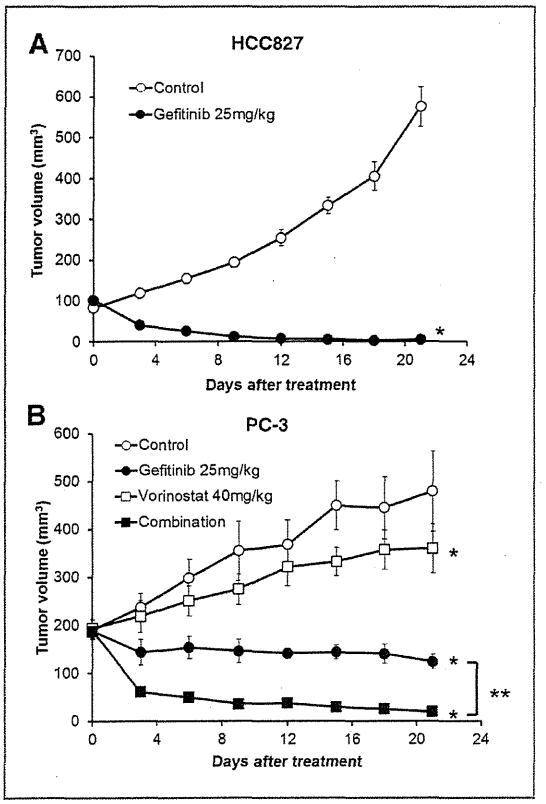

Figure 3. Antitumor activity of gefitinib and/or vorinostat in mouse xenograft models of HCC827 and PC-3 tumors. Nude mice bearing established tumors with HCC827 (A) or PC-3 (B) cells were treated with 25 mg/kg gefitinib and/or 40mg/kg vorinostat once daily for 21 days. Tumor volume was measured using calipers on the indicated days. Mean ± SE tumor volumes are shown for groups of 4 to 5 mice. *, $P < 0.05$ versus control, **, $P < 0.05$ versus gefitinib by one-way ANOVA.

Discussion

EGFR-mutant NSCLC cells with the *BIM* deletion polymorphism show impaired generation of BIM with the proapoptotic BH3 domain, as well as resistance to EGFR-TKI–induced apoptosis (5). We have shown here that treatment of cells with the combination of vorinostat, a HDAC inhibitor, and gefitinib, an EGFR-TKI, restored the expression of BIM protein with a BH3 domain (predominantly BIM_{EL}), induced apoptosis, and overcame gefitinib resistance *in vitro* and *in vivo*.

Although vorinostat preferentially induced expression of BIM containing the BH3 domain, its exact mechanisms of action remain unclear. The wild-type allele may be more susceptible to the effects of HDAC inhibition than the deletion allele due to differences in the acetylation status of these alleles. Alternatively, vorinostat may affect the splicing process, resulting in the production of exon 4- rather than exon 3-containing transcripts from the deletion polymorphism allele as HDAC has been found to affect the splicing of RNA (16).

Vorinostat has been shown to induce the expression of several genes other than *BIM* (13). However, we found that BIM was pivotal not only for gefitinib-induced apoptosis but also when combined with vorinostat. Moreover, the combination of vorinostat and gefitinib increased BIM expression and markedly induced apoptosis in PC-3 and HCC2279 cells. Collectively, these findings strongly suggest that vorinostat promotes gefitinib-induced apoptosis in *EGFR*-mutant NSCLC cells with the *BIM* polymorphism, primarily by increasing BIM expression. Several other mechanisms, including inhibition of epigenetic modifications leading to a drug-tolerant state (17) and transition of cancer cells from a resistant mesenchymal state to an E-cadherin–expressing epithelial state (18) may be also involved.

Both the *BIM* polymorphism and *EGFR* mutations are more prevalent in East Asian than in Caucasian populations. Few East Asian patients with *EGFR*-mutant NSCLC show a complete response to EGFR-TKIs (1). This incomplete response, including intrinsic resistance, may be due, in part, to low BIM expression associated with the *BIM* polymorphism (6). Our preclinical data indicate that vorinostat increases BIM even in *BIM*-wild type *EGFR*--mutant NSCLC cells. However, a clinical trial with erlotinib and entinostat, an HDAC inhibitor, in

Published OnlineFirst February 4, 2013; DOI: 10.1158/0008-5472.CAN-12-3479

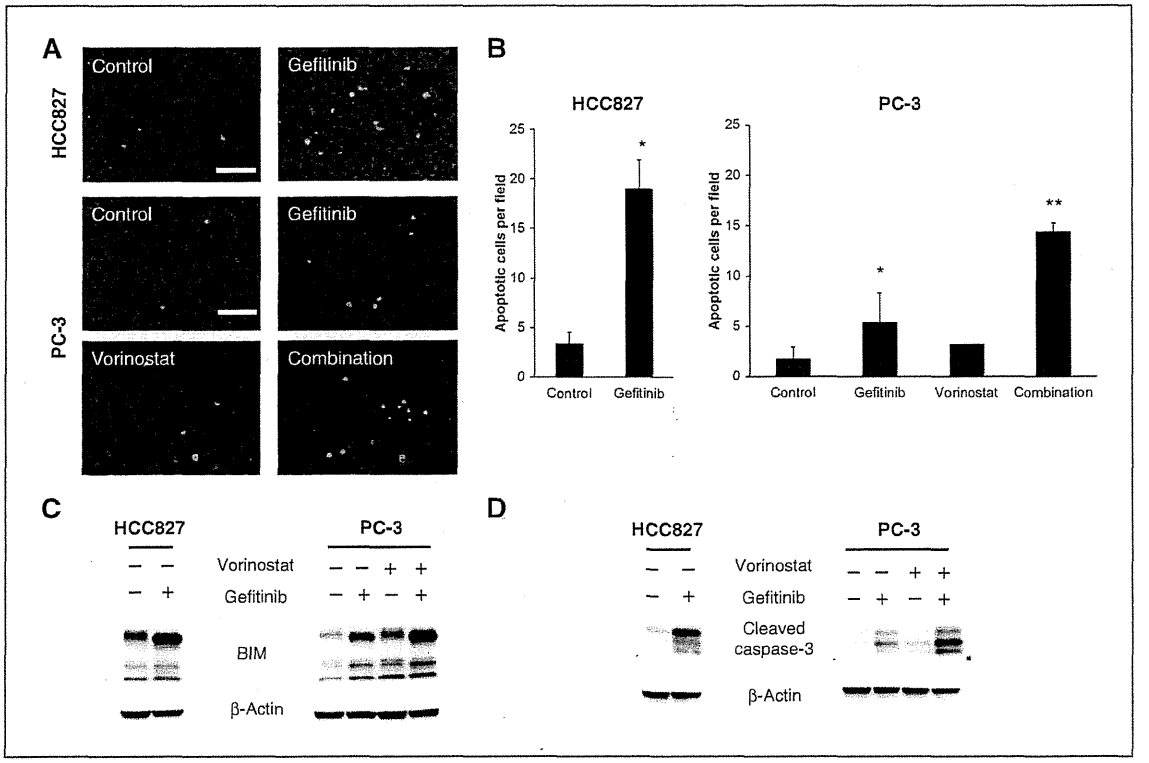

Figure 4. Vorinostat combined with gefitinib increases apoptosis in xenograft tumors with the *BIM* polymorphism. HCC827 and PC-3 xenograft tumors were resected from mice treated with 25 mg/kg gefitinib and/or 40mg/kg vorinostat for 4 days. A, analysis of apoptosis by TUNEL staining. Representative fluorescent images are shown. Green fluorescence indicates apoptotic cells. Bar indicates 50 μm. B, quantitation of number of apoptotic cells. *, $P < 0.05$ gefitinib or vorinostat versus control; **, $P < 0.05$ combination versus control and single agents. Bars represent mean ± SD. C, tumors were harvested 8 hours after 2 consecutive treatments with each compound, and the levels of protein in tumor lysates were determined by Western blotting. D, tumors were harvested 24 hours after 4 consecutive treatments with each compound. Protein expression levels in the tumor lysates were determined by Western blotting.

unselected patients with NSCLC, more than 65% of whom were Caucasian, failed to show therapeutic benefits (19). These findings suggest that the combination of vorinostat and an EGFR-TKI should be tested in selected patients with NSCLC with *EGFR* mutations and the *BIM* polymorphism.

Resistance to EGFR-TKIs associated with the *BIM* deletion polymorphism may be overcome by treatment with BH3 mimetics, such as ABT-737 (5). Although ABT-737 antagonized antiapoptotic proteins, such as Bcl-2 and Bcl-X_L, it did not antagonize the antiapoptotic protein Mcl-1, which is overexpressed in NSCLC (20), suggesting that the effects of BH3 mimetics may be limited to overcoming EGFR-TKI resistance caused by the *BIM* polymorphism in NSCLC. BH3 mimetics are being evaluated in early-phase clinical trials but are not ready for use in clinical practice. In contrast, vorinostat has been approved by the FDA for the treatment of patients with advanced primary cutaneous T-cell lymphoma (15). Therefore, the combination of gefitinib and vorinostat could easily be tested clinically.

The *BIM* polymorphism can be detected in formalin-fixed paraffin-embedded tumor tissues and peripheral blood (5). Moreover, a convenient and easy access PCR screening method can detect this polymorphism in circulating DNA from serum (Supplementary Fig. S5A and S5B). As the *BIM* polymorphism is a germline alteration, it can be assayed in serum obtained at any time point. Collectively, our findings illustrate the importance of clinical trials testing the ability of combinations of vorinostat and EGFR-TKIs to overcome EGFR-TKI resistance associated with the *BIM* polymorphism in patients with *EGFR*--mutant NSCLC.

Disclosure of Potential Conflicts of Interest

T. Nakagawa is an employee of Eisai Co., Ltd. for oncology research. Y. Hasegawa received research funding from Chugai Pharmaceutical Co., Ltd., Merck Sharp & Dohme Corp., AstraZeneca, and TAIHO Pharmaceutical Co., Ltd. S. Yano received honoraria from Chugai Pharmaceutical Co., Ltd. and AstraZeneca and received research funding from Chugai Pharmaceutical Co., Ltd., Kyowa Hakko Kirin Co., Ltd., and Eisai Co., Ltd. No potential conflicts of interest were disclosed by the other authors.

Authors' Contributions

Conception and design: T. Nakagawa, S. Takeuchi, S. Nanjo, S. Yano
Development of methodology: T. Nakagawa, S. Takeuchi
Acquisition of data (provided animals, acquired and managed patients, provided facilities, etc.): T. Nakagawa, D. Ishikawa, Y. Hasegawa

Published OnlineFirst February 4, 2013; DOI: 10.1158/0008-5472.CAN-12-3479

Analysis and interpretation of data (e.g., statistical analysis, biostatistics, computational analysis): T. Nakagawa, S. Yano
Writing, review, and/or revision of the manuscript: T. Nakagawa, S. Takeuchi, H. Ebi, M. Sato, Y. Hasegawa, Y. Sekido, S. Yano
Administrative, technical, or material support (i.e., reporting or organizing data, constructing databases): T. Yamada, T. Sano, M. Sato, Y. Sekido
Study supervision: S. Takeuchi, Y. Sekido, S. Yano

Acknowledgments

The authors thank Dr. John Minna (University of Texas Southwestern Medical Center) for the HCC2279 cells.

Grant Support

This study was supported by Grants-in-Aid for Cancer Research (21390256 to S. Yano; 11019957 to S. Takeuchi), Scientific Research on Innovative Areas "Integrative Research on Cancer Microenvironment Network" (22112010A01 to S. Yano), and Grant-in-Aid for Project for Development of Innovative Research on Cancer Therapeutics (P-Direct) from the Ministry of Education, Culture, Sports, Science, and Technology (MEXT) of Japan.

Received September 3, 2012; revised December 20, 2012; accepted January 19, 2013; published OnlineFirst February 4, 2013.

References

1. Maemondo M, Inoue A, Kobayashi K, Sugawara S, Oizumi S, Isobe H, et al.North-East Japan Study Group. Gefitinib or chemotherapy for non-small-cell lung cancer with mutated EGFR. N Engl J Med 2010;362:2380–8.
2. Pao W, Chmielecki J. Rational, biologically based treatment of EGFR-mutant non-small-cell lung cancer. Nat Rev Cancer 2010;10:760–74.
3. Sequist LV, Waltman BA, Dias-Santagata D, Digumarthy S, Turke AB, Fidias P, et al. Genotypic and histological evolution of lung cancers acquiring resistance to EGFR inhibitors. Sci Transl Med 2011; 3:75ra26.
4. Yano S, Wang W, Li Q, Matsumoto K, Sakurama H, Nakamura T, et al. Hepatocyte growth factor induces gefitinib resistance of lung adenocarcinoma with epidermal growth factor receptor-activating mutations. Cancer Res 2008;68:9479–87.
5. Ng KP, Hillmer AM, Chuah CT, Juan WC, Ko TK, Teo AS, et al. A common BIM deletion polymorphism mediates intrinsic resistance and inferior responses to tyrosine kinase inhibitors in cancer. Nat Med 2012;18:521–8.
6. O'Connor L, Strasser A, O'Reilly LA, Hausmann G, Adams JM, Cory S, et al. Bim: a novel member of the Bcl-2 family that promotes apoptosis. EMBO J 1998;17:384–95.
7. Chen L, Willis SN, Wei A, Smith BJ, Fletcher JI, Hinds MG, et al. Differential targeting of prosurvival Bcl-2 proteins by their BH3-only ligands allows complementary apoptotic function. Mol Cell 2005;17: 393–403.
8. Heath-Engel HM, Shore GC. Regulated targeting of Bax and Bak to intracellular membranes during apoptosis. Cell Death Differ 2006;13: 1277–80.
9. Costa DB, Halmos B, Kumar A, Schumer ST, Huberman MS, Boggon TJ, et al. BIM mediates EGFR tyrosine kinase inhibitor-induced apoptosis in lung cancers with oncogenic EGFR mutations. PLoS Med 2007;4:1669–79.
10. Fukazawa H, Noguchi K, Masumi A, Murakami Y, Uehara Y. BimEL is an important determinant for induction of anoikis sensitivity by mitogen-activated protein/extracellular signal-regulated kinase kinase inhibitors. Mol Cancer Ther 2004;3:1281–8.
11. Liu JW, Chandra D, Tang SH, Chopra D, Tang DG. Identification and characterization of Bimgamma, a novel proapoptotic BH3-only splice variant of Bim. Cancer Res 2002;62:2976–81.
12. Faber AC, Corcoran RB, Ebi H, Sequist LV, Waltman BA, Chung E, et al. BIM expression in treatment-naive cancers predicts responsiveness to kinase inhibitors. Cancer Discov 2011;1:352–65.
13. Bolden JE, Peart MJ, Johnstone RW. Anticancer activities of histone deacetylase inhibitors. Nat Rev Drug Discov 2006;5:769–84.
14. Mann BS, Johnson JR, Cohen MH, Justice R, Pazdur R. FDA approval summary: vorinostat for treatment of advanced primary cutaneous T-cell lymphoma. Oncologist 2007;12:1247–52.
15. Xargay-Torrent S, Lopez-Guerra M, Saborit-Villarroya I, Rosich L, Campo E, Roue G, et al. Vorinostat-induced apoptosis in mantle cell lymphoma is mediated by acetylation of proapoptotic BH3-only gene promoters. Clin Cancer Res 2011;17:3956–68.
16. Delcuve GP, Khan DH, Davie JR. Roles of histone deacetylases in epigenetic regulation: emerging paradigms from studies with inhibitors. Clin Epigenetics 2012;4:5.
17. Sharma SV, Lee DY, Li B, Quinlan MP, Takahashi F, Maheswaran S, et al. A chromatin-mediated reversible drug-tolerant state in cancer cell subpopulations. Cell 2010;141:69–80.
18. Witta SE, Gemmill RM, Hirsch FR, Coldren CD, Hedman K, Ravdel L, et al. Restoring E-cadherin expression increases sensitivity to epidermal growth factor receptor inhibitors in lung cancer cell lines. Cancer Res 2006;66:944–50.
19. Witta SE, Jotte RM, Konduri K, Neubauer MA, Spira AI, Ruxer RL, et al. Randomized phase II trial of erlotinib with and without entinostat in patients with advanced non-small-cell lung cancer who progressed on prior chemotherapy. J Clin Oncol 2012;30:2248–55.
20. Cetin Z, Ozbilim G, Erdogan A, Luleci G, Karauzum SB. Evaluation of PTEN and Mcl-1 expressions in NSCLC expressing wild-type or mutated EGFR. Med Oncol 2010;27:853–60.

Cancer Science
The official journal of the Japanese Cancer Association JCA

Cancer-associated missense mutations of caspase-8 activate nuclear factor-κB signaling

Mizuo Ando,[1,2] Masahito Kawazu,[1] Toshihide Ueno,[3] Kazutaka Fukumura,[1] Azusa Yamato,[3] Manabu Soda,[3] Yoshihiro Yamashita,[3] Young L. Choi,[1] Tatsuya Yamasoba[2] and Hiroyuki Mano[1,3,4,5,6]

Departments of [1]Medical Genomics; [2]Otolaryngology and Head and Neck Surgery, Graduate School of Medicine, University of Tokyo, Tokyo; [3]Division of Functional Genomics, Jichi Medical University, Tochigi; [4]Department of Cellular Signaling, Graduate School of Medicine, University of Tokyo, Tokyo; [5]CREST, Japan Science and Technology Agency, Saitama, Japan

(Received December 7, 2012/Revised April 26, 2013/Accepted May 6, 2013/Accepted manuscript online May 9, 2013/Article first published online June 7, 2013)

Head and neck squamous cell carcinoma (HNSCC) is an aggressive cancer with a 5-year survival rate of ~50%. With the use of a custom cDNA-capture system coupled with massively parallel sequencing, we have now investigated transforming mechanisms for this malignancy. The cDNAs of cancer-related genes (n = 906) were purified from a human HNSCC cell line (T3M-1 Cl-10) and subjected to high-throughput resequencing, and the clinical relevance of non-synonymous mutations thus identified was evaluated with luciferase-based reporter assays. A CASP8 (procaspase-8) cDNA with a novel G-to-C point mutation that results in the substitution of alanine for glycine at codon 325 was identified, and the mutant protein, CASP8 (G325A), was found to activate nuclear factor-κB (NF-κB) signaling to an extent far greater than that achieved with the wild-type protein. Moreover, forced expression of wild-type CASP8 suppressed the growth of T3M-1 Cl-10 cells without notable effects on apoptosis. We further found that most CASP8 mutations previously detected in various epithelial tumors also increase the ability of the protein to activate NF-κB signaling. Such NF-κB activation was shown to be mediated through the COOH-terminal region of the second death effector domain of CASP8. Although CASP8 mutations associated with cancer have been thought to promote tumorigenesis as a result of attenuation of the proapoptotic function of the protein, our results now show that most such mutations, including the novel G325A identified here, separately confer a gain of function with regard to activation of NF-κB signaling, indicating another role of CASP8 in the transformation of human malignancies including HNSCC. (*Cancer Sci* 2013; 104: 1002–1008)

Head and neck squamous cell carcinoma (HNSCC) is one of the most common types of human cancer, with an annual incidence of more than 500 000 cases worldwide.[1,2] The major risk factors for HNSCC are tobacco use, alcohol consumption, and infection with human papilloma virus.[3] It is an aggressive cancer with a propensity for local invasion and metastasis, which directly leads to disease- or treatment-related morbidity. The goals of HNSCC treatment are therefore not only to improve survival outcome but also to preserve vital physiological functions such as speech, breathing, swallowing, and hearing.

Most patients with HNSCC, however, present with advanced disease at the time of first evaluation and have a 5-year survival rate of only ~50%. Although advances in surgery and chemoradiation treatment have helped to preserve organ function in such individuals, they have resulted in only a moderate improvement in patient survival during the past 30 years. Characterization of the molecular mechanisms of HNSCC oncogenesis is expected to provide important information for the development of novel anticancer agents and the identification of biomarkers.

The recent advent of massively parallel sequencers, or next-generation sequencers, has rendered resequencing of the cancer genome manageable in private laboratories.[4] We have recently shown that a custom cDNA-capture system coupled with massively parallel sequencing provides a feasible and relatively simple approach for the simultaneous detection of point mutations, insertions/deletions (indels), and gene fusions among the captured genes.[5] Here we show that such high-throughput resequencing of targeted cDNAs from an oral squamous cell carcinoma cell line led to the identification of a missense mutation in caspase-8 (CASP8), a member of the cysteine–aspartic acid protease (caspase) family. Unexpectedly, CASP8 with this amino acid substitution (glycine-325 to alanine, or G325A) was found to activate signaling by the antiapoptotic transcription factor nuclear factor-κB (NF-κB) to an extent markedly greater than that observed with the wild-type protein. Of interest, most CASP8 mutants previously identified in human cancers were also found to activate the NF-κB pathway. As far as we are aware, a direct antiapoptotic effect of CASP8 in cancer has not previously been demonstrated.

Materials and Methods

Cell lines and plasmids. Human embryonic kidney 293T (HEK293T) cells, human oral squamous cell carcinoma T3M-1 Cl-10 cells, and human esophageal squamous cell carcinoma OE21 cells were obtained from RIKEN Cell Bank (Tsukuba, Japan), ATCC (Manassas, VA, USA), and European Collection of Cell Cultures (Salisbury, UK), respectively. All cells were maintained in DMEM–F12 supplemented with 10% FBS and 2 mM L-glutamine (all of which were from Invitrogen, Carlsbad, CA, USA). A full-length cDNA for the G325A mutant form of CASP8 was isolated by RT-PCR from T3M-1 Cl-10 cells and inserted into the retroviral plasmid pMXS.[6] Expression vectors for wild-type and previously identified mutant forms of CASP8 were generated by PCR-based mutagenesis. The nucleotide sequences of all constructs were confirmed by Sanger sequencing.

Resequencing coupled with a cDNA-capture system. Resequencing coupled with a custom cDNA-capture system was carried out as described previously.[5] In brief, RNA capture probes (Agilent Technologies, Santa Clara, CA, USA) designed to cover cDNAs of 906 human protein-coding genes were hybridized with cDNA fragments prepared from T3M-1 Cl-10 cells according to the protocols for the SureSelect Target Enrichment system (Agilent Technologies). Purified cDNA fragments were then subjected to deep sequencing for 76 bases from both ends with a Genome Analyzer IIx (GAIIx; Illumina, San Diego, CA, USA). Reads with a Q-value ≥20 at every

[6]To whom correspondence should be addressed.
E-mail: hmano@m.u-tokyo.ac.jp

doi: 10.1111/cas.12191

base were selected, and mapped to the reference cDNA sequences as well as the human genome sequence (GRCh37) with the Bowtie algorithm.[7] After removing single nucleotide polymorphisms (dbSNP build 32; http://www.ncbi.nlm.nih.gov/projects/SNP/snp_summary.cgi), non-synonymous mutations (≥30% mutation ratio at ≥30× coverage) for the target cDNAs were isolated by our in-house pipeline.

Luciferase-based reporter assays. The HEK293T cells were transfected with a CASP8 expression vector, the pGL-TK plasmid (Promega, Madison, WI, USA), and a luciferase-based reporter plasmid for signaling by c-Fos (pFL700),[8] c-Myc (pHXL),[9] β-catenin (TOP-flash; Upstate Biotechnology, Lake Placid, NY, USA), JNK (AP1; Panomics, Santa Clara, CA, USA), TP53,[10] Notch (pGa981-6),[11] Rho (pSRE.L),[12] MAPK (ELK1; Panomics), Gli (Genentech, South San Francisco, CA, USA), or NF-κB (Agilent Technologies). Luciferase activities were then assayed with a Dual-Luciferase Reporter Assay System (Promega), and the activity of firefly luciferase was normalized by that of *Renilla* luciferase.

Apoptosis and cell proliferation assays. The T3M-1 Cl-10 cells, which express CASP8(G325A), and OE21 cells, which express wild-type CASP8, were infected with a retrovirus generated from the pMXS-CASP8-ires-EGFP vector (Clontech, Mountain View, CA, USA), which allows simultaneous expression of CASP8 and enhanced green fluorescent protein (EGFP). The cells were then collected and assayed for apoptosis by staining with annexin V and propidium iodide (eBioscience, San Diego, CA, USA) followed by flow cytometry (FACSCanto II instrument; BD Biosciences, San Jose, CA, USA). Cell apoptosis was quantified by the Click-iT TUNEL Alexa Fluor Imaging Assay (Invitrogen). Cell proliferation was assayed by flow cytometric determination of the cell fraction positive for EGFP.

Statistical analysis. Quantitative data are presented as means ± SD and were compared with Student's *t*-test. A *P*-value of <0.05 was considered statistically significant.

Results

Identification of a CASP8 mutation in T3M-1 Cl-10 cells. To identify oncogenes for oral squamous cell carcinoma, we selected cDNA fragments for cancer-related genes (n = 906) from T3M-1 Cl-10 oral squamous cell carcinoma cells with the use of our custom cDNA-capture system.[5] Deep sequencing of such fragments with a GAIIx sequencer yielded 91 961 299 independent high-quality reads that mapped to 850 cDNAs with a mean coverage of 1202 reads/bp. Screening for missense mutations, indels, and gene fusions with our in-house computational pipeline resulted in the identification of 12 non-synonymous mutations that were further confirmed by Sanger sequencing (Table 1). We did not detect any indels or gene fusions that were confirmed by the capillary sequencing.

The 12 missense mutations include a novel G-to-C change at position 1183 of *CASP8* cDNA (GenBank accession number, NM_033355.3), which results in a glycine-to-alanine substitution at codon 325 of the encoded protein (Fig. 1a), as well as known HNSCC-related mutations such as those in *TP53* and *HRAS*. In our deep sequencing data, this substituted position of *CASP8* cDNA was read at a depth of ×469 and showed a mutation ratio of 98.5%, indicative of loss of heterozygosity at this locus.

The *CASP8* gene encodes the inactive (pro) form of CASP8, which plays an essential role in the execution of apoptosis.[13] Caspase-8 is composed of a COOH-terminal catalytic domain and an NH_2-terminal prodomain region that contains two tandem death effector domains (DEDs) (Fig. S1). Activation of CASP8 requires autoproteolysis that generates a heterodimer consisting of large (p20) and small (p10) protease subunits. The G325A mutation of CASP8 is located near the catalytic site in the p20 subunit.

Mutant CASP8(G325A) activates the NF-κB signaling pathway. To evaluate the biological relevance of the CASP8 (G325A) mutant, we carried out a reporter assay for a wide range of intracellular signaling pathways. Wild-type CASP8 markedly increased reporter activity for the NF-κB pathway (Fig. 1b), consistent with previous observations.[14,15] The G325A mutant of CASP8, however, increased such reporter activity to an extent far greater than that observed with the wild-type protein. In contrast, the effects of the wild-type and mutant forms of CASP8 on other signaling pathways, including those mediated by c-Fos, c-Myc, β-catenin, JNK, TP53, Notch, Rho, MAPK, and Gli, did not differ significantly (Fig. 1c), indicating that the G325A mutation influences NF-κB signaling specifically.

Catalytic activity of CASP8 and its mutants was also examined. The wild-type CASP8, CASP8(G325A), CASP8(C360A) (an amino acid substitution at the catalytic center),[16] CASP8 (D210A/D216A) (double mutations at the autoprocessing region), or CASP8(D210A/D216A/D223A) (triple mutations at the autoprocessing region), was introduced into HEK293 cells that were then subjected to an enzymatic assay for CASP8. As expected, wild-type CASP8 is catalytically active in HEK293, but a mutation at its catalytic center almost abolished its processing potency (Fig. 2a). Interestingly, the G325A substitution severely hampered CASP8 activity. In contrast, CASP8 with mutations at the autoprocessing region carry a decreased, but apparent, processing ability.

To examine whether the G350A mutation contributes directly to malignant transformation, we infected T3M-1 Cl-10 cells harboring the mutant *CASP8* gene with a retrovirus encoding both EGFP and either wild-type CASP8 or the

Table 1. Non-synonymous mutations detected in T3M-1 Cl-10 cells

Gene	GenBank accession no.	Read coverage	Mismatch reads (%)	Nucleotide change	Amino acid change
CASP8	NM_033355	×469	98.5	1183G>C	G325A
ELF4	NM_001421	×188	39.8	1016C>A	L211M
GSG2	NM_031965	×119	100.0	1238T>C	V402A
HRAS	NM_005343	×613	25.1	370A>T	Q61L
IRAK2	NM_001570	×155	49.0	591C>T	S172L
NUAK2	NM_030952	×162	51.2	1427G>A	A434T
PDPK1	NM_002613	×226	37.6	1663G>C	E507Q
PRKCZ	NM_002744	×61	49.1	306C>T	R49C
PXK	NM_017771	×82	57.3	364A>G	I89V
RHOA	NM_001664	×1127	52.9	394G>C	E40Q
TP53	NM_000546	×234	97.8	1035A>G	R280G
TTBK2	NM_173500	×100	51.0	1402G>C	L321F

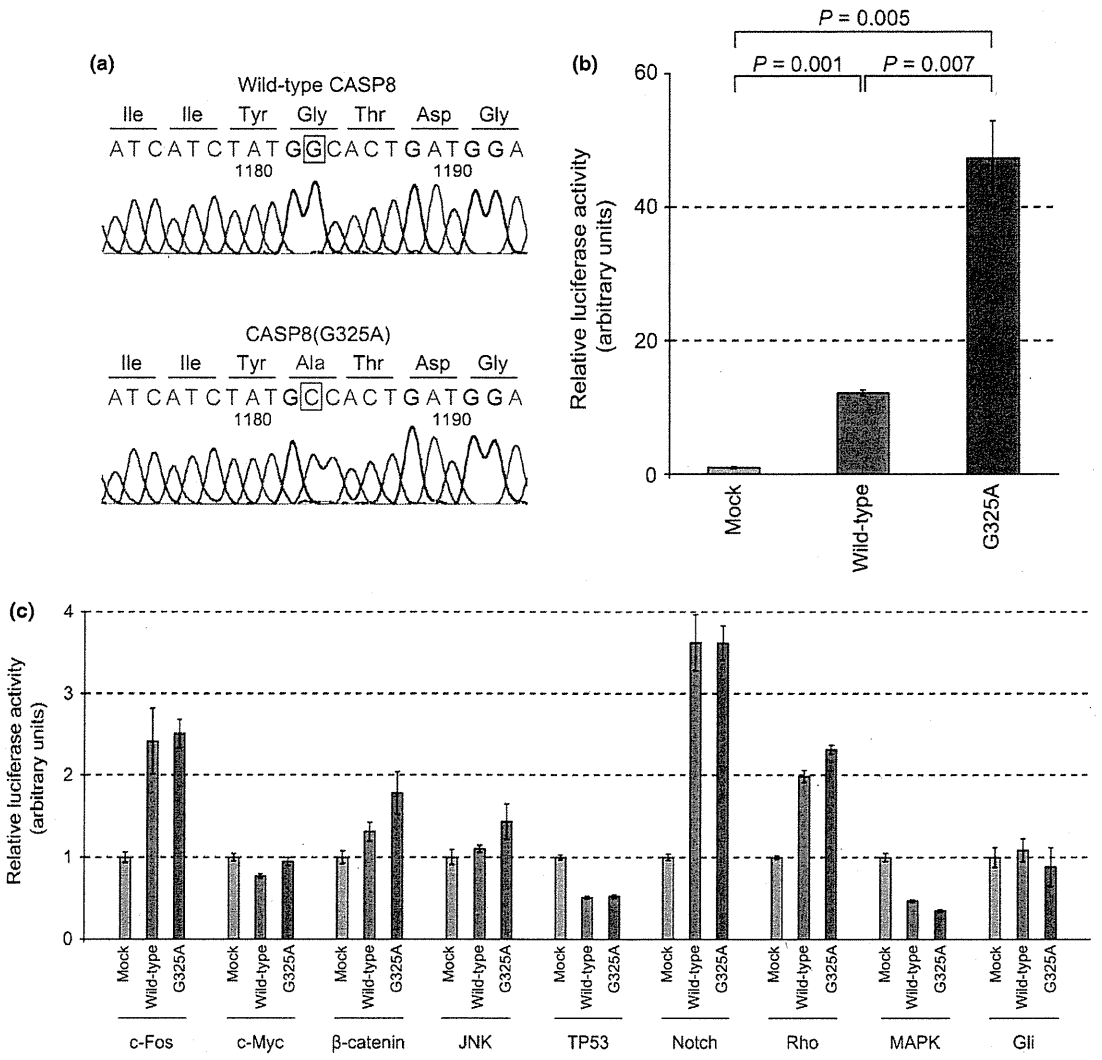

Fig. 1. Mutant protein CASP8(G325A) selectively activates the nuclear factor-κB (NF-κB) signaling pathway. (a) Electrophoretograms of *CASP8* cDNA identified an 1183G > C substitution, which results in a G325A amino acid substitution, in T3M-1 Cl-10 cells. (b,c) HEK293T cells were transfected with an expression vector for CASP8 or CASP8(G325A) or with the corresponding empty vector (Mock) together with pGL-TK and reporter plasmids for NF-κB (b) or other (c) signaling pathways, after which the cells were lysed and assayed for luciferase activities. The activity of firefly luciferase was normalized by that of *Renilla* luciferase then expressed relative to the corresponding value for mock-transfected cells. Data are means ± SD from three independent experiments. *P*-values were calculated using Student's *t*-test.

G325A mutant, then assayed the proliferation of EGFP-positive cells. Surprisingly, forced expression of wild-type CASP8 resulted in a marked reduction in the number of EGFP-positive cells, whereas the G325A mutant had only a slight effect on cell number (Fig. 2b). This suppression of cell growth by wild-type CASP8 was not observed in another squamous cell carcinoma cell line, OE21, which harbors the wild-type *CASP8* gene (Fig. 2b).

Interestingly, while annexin V-positive fraction was marginally increased in T3M-1 Cl-10 cells overexpressing wild-type CASP8 (Fig. S2), neither CASP8 nor CASP8 (G325A) induced notable apoptosis in T3M-1 Cl-10, as judged by the TUNEL assay (Fig. 2c). It is, therefore, possible that CASP8 regulation of cell growth in cancer may be independent, in part, of its apoptosis-inducing function.

We further depleted the *CASP8* message in T3M-1 Cl-10 by the use of siRNA, and examined its effects on the expression of NF-κB targets. As shown in Figure S3, decrease in the *CASP8* message led to a marked suppression in *BCL2* expression, supporting the positive role of CAPS8 in NF-κB signaling.

CASP8 mutations in human tumors. Non-synonymous mutations in CASP8 have been previously reported in various epithelial tumor types including gastric cancer (GC), colorectal cancer, hepatocellular carcinoma, and HNSCC.[16–19] These mutations include seven missense, one nonsense, and six frameshift mutations as well as one in-frame deletion (Fig. S1, Table S1). Whereas such mutations have been thought to contribute to carcinogenesis through a loss of the proapoptotic function of CASP8, we unexpectedly found that most of the mutants markedly activated NF-κB signaling (Fig. 3), suggestive of a gain of function with regard to such signaling. Of note, all of the three CASP8 mutants (GC1, GC4, and GC7) that failed to activate NF-κB signaling harbor non-synonymous mutations within the DEDs, suggesting that these domains may be essential for NF-κB activation.

In addition, screening as of January 2013 for non-synonymous mutations in CASP8 among public databases for

doi: 10.1111/cas.12191

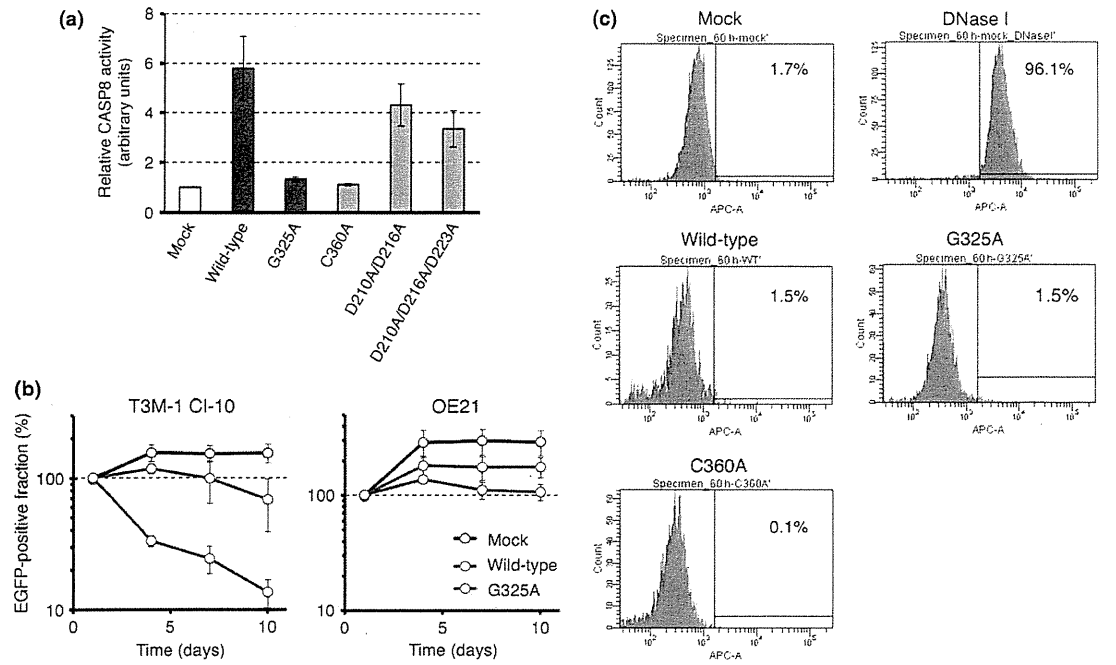

Fig. 2. Caspase-8 (CASP8) suppresses the proliferation of T3M-1 Cl-10 cells but not that of OE21 cells. (a) Proteolytic activity of CASP8 was measured with the Caspase-Glo8 assay for HEK293 cells expressing wild-type CASP8, CASP8(G325A), CASP8(C360A), CASP8(D210A/D216A), or CASP8(D210A/D216A/D223A), and is shown relative to the value for mock-transfected cells. Data are means ± SD from three independent experiments. (b) T3M-1 Cl-10 cells (left panel) or OE21 cells (right panel) were infected with a retrovirus encoding enhanced green fluorescent protein (EGFP) either alone (Mock) or together with wild-type or G325A mutant forms of CASP8. The number of EGFP-positive cells was then measured by flow cytometry at 1, 4, 7, and 10 days after infection and is expressed as a percentage of that at 1 day after infection. Data are means ± SD from three independent experiments. (c) Fragmented DNA in apoptotic cells was quantified by TUNEL assay for T3M-1 Cl-10 cells infected with an empty virus (Mock), or virus expressing wild-type, G325A mutant, or C360A mutant of CASP8. Fractions of cells with fragmented DNA are indicated as percentages. T3M-1 Cl-10 cells treated with DNase I were used as a positive control of apoptosis.

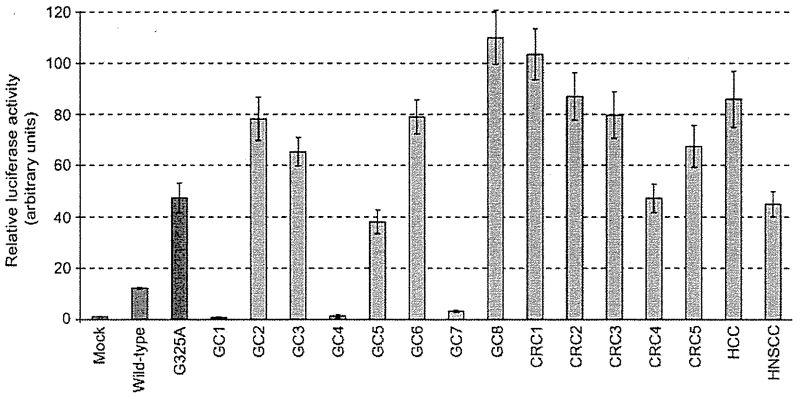

Fig. 3. Tumor-associated caspase-8 (CASP8) mutants activate the nuclear factor-κB pathway. HEK293T cells were transfected with a luciferase reporter plasmid for nuclear factor-κB, with pGL-TK, and with expression vectors for wild-type or the indicated mutant forms of CASP8. Normalized firefly luciferase activity was then determined and expressed relative to the value for mock-transfected cells. Data are means ± SD from three independent experiments. CRC, colorectal cancer; GC, gastric cancer; HCC, hepatocellular carcinoma; HNSCC, head and neck squamous cell carcinoma.

cancer genome mutations (COSMIC version 62, http://cancer.sanger.ac.uk/cancergenome/projects/cosmic/; The Cancer Genome Atlas, https://tcga-data.nci.nih.gov/tcga/tcgaHome2.jsp; and the International Cancer Genome Consortium, http://icgc.org) list 76 independent missense/nonsense mutations, seven frame-shift indels within CASP8, many of which had been confirmed to be somatic changes. Interestingly, amino acid substitutions at Gly-325 (including G325A) were identified in multiple cancer specimens (such as those for large intestine carcinoma and cervical squamous cell carcinoma), suggesting that missense mutations at this position are recurrent.

Caspase-8 domains linked to NF-κB activation. To investigate further how CASP8 controls the NF-κB pathway, we generated a series of CASP8 mutants (Fig. 4a). As shown in Figure 4(b), the D210A/D216A mutant is still able to activate NF-κB signaling by an extent similar to that achieved with the wild-type protein. Similarly, the addition of both D210A and D216A

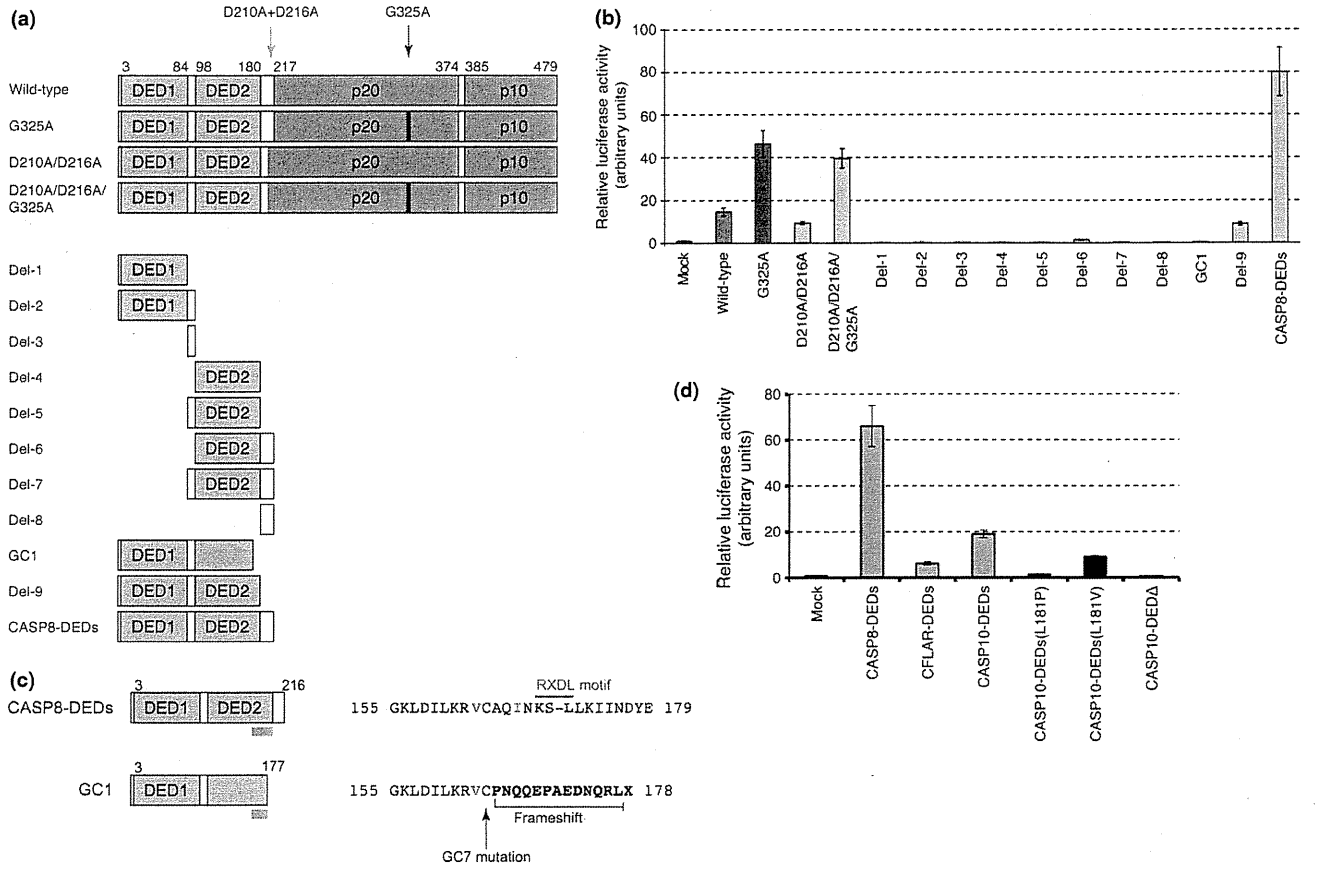

Fig. 4. Death effector domains (DEDs) activate nuclear factor-κB (NF-κB) signaling. (a) The protein structure of caspase-8 (CASP8) mutants is shown schematically with amino acid numbers indicated at the top. In addition to the wild-type and D210A/D216A mutant forms with or without the G325A substitution, various constructs for the DED and Hinge regions (Del-1 to Del-9) were generated. The structure of the mutant from cancer specimen GC1 and a mutant encompassing both DEDs and Hinge regions (CASP8-DEDs) is also shown. (b) Expression plasmids for the CASP8 mutants in (A) were introduced into HEK293T cells for the NF-κB reporter assay. Normalized firefly luciferase activity is expressed relative to the value for mock-transfected cells. Data are means ± SD from three independent experiments. (c) Amino acid sequences of the COOH-terminal regions (depicted by light blue bars in the left panel) of CASP8-DEDs and the CASP8 mutant from specimen GC1 are shown at the right. The conserved RXDL motif is indicated in red, and Val^{163} and Ile^{167} residues that contribute to the conserved hydrophobic patch are indicated in green. In the GC1 mutant, a frameshift deletion changes the amino acid sequence after Cys^{164} and generates a termination codon. The GC7 mutant has a C164Y substitution that markedly attenuates CASP8-induced NF-κB activation. (d) The ability to activate the NF-κB pathway was examined for CASP8-DEDs and the corresponding regions of CFLAR (amino acid residues 1–196) and CASP10 (residues 1–219), as in (b). For CASP10, we also examined the DED region with a L181P or L181V substitution, or RXDL-deleted DEDΔ encompassing only amino acid residues 1–175.

substitutions to CASP8(G325A) did not substantially affect its ability to activate the NF-κB pathway.

We also generated expression constructs for the NH_2-terminal DED (DED1) or COOH-terminal DED (DED2) either alone or together with the Hinge regions between DED1 and DED2 (Hinge-1) or between DED2 and p20 (Hinge-2) (Fig. 4a). None of these deletion mutants activated the NF-κB pathway (Fig. 4b). In contrast, a deletion mutant consisting of the entire prodomain (CASP8-DEDs) activated NF-κB signaling to a level even higher than that induced by CASP8 (G325A). Deletion of Hinge-2 from CASP8-DEDs (the Del-9 mutant) markedly reduced the stimulatory effect on NF-κB signaling. A *CASP8* cDNA previously identified in the specimen designated GC1 has a 2-bp deletion (Table S1) that results in premature termination within DED2 (Fig. 4c). This truncation almost completely abrogated the ability of CASP8 to activate NF-κB signaling (Figs 3,4b). Both Hinge-2 and the COOH-terminal end of DED2 thus likely play an essential role in the regulation of NF-κB signaling by CASP8. This notion was reinforced by the observation that a Cys^{164}-to-Tyr substitution at the COOH-terminal end of DED2 previously identified in the GC7 specimen (Table S1, Fig. 4c) also largely abolished the ability of CASP8 to activate NF-κB signaling (Fig. 3).

Members of the DED family of proteins possess a key hydrophobic patch (for DED–DED interactions) that is exposed at the surface of each molecule and includes the conserved RXDL motif (corresponding to "KS – L" in DED2 of CASP8) in the COOH-terminal region of the DED.[20–22] Our findings are thus consistent with the idea that this conserved region contributes to the regulation of NF-κB.

Prodomains of CASP8-related proteins are able to activate NF-κB signaling. Given that the prodomain of CASP8 is sufficient to fully active NF-κB signaling, we tested whether the prodomains of the CASP8-related proteins CFLAR (also known as cFLIPL) and caspase-10 (CASP10) might have similar effects. CFLAR is structurally similar to CASP8 but does not possess functional caspase activity, given that it does not

doi: 10.1111/cas.12191

contain the conserved catalytic cysteine residue found in all functional caspases.[23] Caspase-10 is highly homologous to CASP8 and is also recruited to, and becomes activated by, death receptors.[24–26] We found that the entire prodomains of CFLAR and CASP10 each markedly increased the level of NF-κB signaling (Fig. 4d) as already shown for CASP10 by other groups.[27] Although conservation of the RXDL motif is less clear in CASP10 compared to the other members (Fig. S4), substitution of the conserved Leu^{181} in CASP10 to either Pro or Val residues attenuated its NF-κB-activating potential (Fig. 4d). Furthermore, the CASP10-DEDs protein lacking the putative RXDL region completely lost such ability, confirming the essential role of the DEDs COOH-terminus in CASP10 activation of the NF-κB pathway.

Discussion

One of the most proximal caspases in the apoptosis cascade, CASP8 is driven by the death-inducing signaling complex in response to ligation of death receptors[13] such as tumor necrosis factor receptor 1, CD95 (Fas, or Apo1), and tumor necrosis factor-related apoptosis-inducing ligand (TRAIL, or Apo2L) receptor. Activation of CASP8 requires dimerization and consequent autocleavage of the procaspase-8 zymogen,[28] and it initiates the extrinsic apoptosis cascade through activation of downstream effectors such as CASP3, CASP6, and CASP7.[29]

In addition, CASP8 has the potential to activate the antiapoptotic transcription factor NF-κB through its tandem DED region,[14,15,30] and IκB kinase γ (IKKγ), an essential regulatory subunit of the IKK complex, participates in this CASP8-mediated activation of NF-κB.[31] The tandem DEDs of CFLAR also directly interact with and recruit IKKγ and thereby activate NF-κB.[32] However, we failed to detect a direct association between the tandem DEDs of CASP8 and IKKγ (data not shown). How the tandem DEDs of CASP8 mediate NF-κB activation thus remains unclear. Given the essential role of the COOH-terminal region of DED2 and the Hinge-2 region of CASP8 in the activation of NF-κB, it will be of interest to profile the cellular proteins that associate with these regions. Importantly, whereas somatic non-synonymous mutations in *CASP8* are detected relatively frequently in human tumors, the mutant proteins have been assumed to accelerate carcinogenesis as a result of a loss of proapoptotic function.[16,18,19]

In contrast, our data now suggest that many of the somatic mutations within *CASP8* in human cancer provide simultaneously inactivation of its proapoptotic function and activation of NF-κB signaling. Additionally, restoration of *CASP8* expression in a *CASP8*-mutant cell line (T3M-1 Cl-10) clearly suppressed cell proliferation without apparent effects on apoptosis, further confirming the relevance of *CASP8* mutation on carcinogenesis. It should be noted, however, that our data does not prove a direct linkage between an enhanced NF-κB signaling and cell growth. It may be possible that CASP8 mutants exert cancer-promoting functions other than the activation of NF-κB pathway.

Importantly, a recent large-scale exome sequencing of HNSCC specimens ($n = 74$) detected somatic mutations of *CASP8* in 8% of tumors,[33] suggestive of an unexpected and transforming role of CASP8 in HNSCC (and maybe also in other epithelial tumors). Whereas activation of NF-κB is frequently detected in a wide array of human malignancies, little is known about the exact mechanisms underlying such activation. Our results show that somatic mutation of *CASP8* may be one such mechanism, and they suggest the possibility of treating *CASP8* mutation-positive tumors with inhibitors of NF-κB, or targeting other proteins that contribute to the NF-κB activation pathway.

Acknowledgments

This study was supported in part by a grant for Research on Human Genome Tailor-made from the Ministry of Health, Labor, and Welfare of Japan, by Grants-in-Aid for Scientific Research (B) from the Japan Society for the Promotion of Science, from The Yasuda Medical Foundation, from The Sagawa Foundation for Promotion of Cancer Research, and from The Mitsubishi Foundation.

Disclosure Statement

The authors have no conflict of interest.

References

1 Mao L, Hong WK, Papadimitrakopoulou VA. Focus on head and neck cancer. *Cancer Cell* 2004; **5**: 311–6.
2 Haddad RI, Shin DM. Recent advances in head and neck cancer. *N Engl J Med* 2008; **359**: 1143–54.
3 Argiris A, Karamouzis MV, Raben D, Ferris RL. Head and neck cancer. *Lancet* 2008; **371**: 1695–709.
4 Mardis ER. A decade's perspective on DNA sequencing technology. *Nature* 2011; **470**: 198–203.
5 Ueno T, Yamashita Y, Soda M *et al.* High-throughput resequencing of target-captured cDNA in cancer cells. *Cancer Sci* 2012; **103**: 131–5.
6 Onishi M, Kinoshita S, Morikawa Y *et al.* Applications of retrovirus-mediated expression cloning. *Exp Hematol* 1996; **24**: 324–9.
7 Langmead B, Trapnell C, Pop M, Salzberg SL. Ultrafast and memory-efficient alignment of short DNA sequences to the human genome. *Genome Biol* 2009; **10**: R25.
8 Hu Q, Milfay D, Williams LT. Binding of NCK to SOS and activation of ras-dependent gene expression. *Mol Cell Biol* 1995; **15**: 1169–74.
9 Takeshita T, Arita T, Higuchi M *et al.* STAM, signal transducing adaptor molecule, is associated with Janus kinase and involved in signaling for cell growth and c-myc induction. *Immunity* 1997; **6**: 449–57.
10 El-Deiry WS, Tokino T, Velculescu VE *et al.* WAF1, a potential mediator of p53 tumor suppression. *Cell* 1993; **75**: 817–25.
11 Kurooka H, Kuroda K, Honjo T. Roles of the ankyrin repeats and C-terminal region of the mouse notch1 intracellular region. *Nucleic Acids Res* 1998; **26**: 5448–55.
12 Hill CS, Wynne J, Treisman R. The Rho family GTPases RhoA, Rac1, and CDC42Hs regulate transcriptional activation by SRF. *Cell* 1995; **81**: 1159–70.
13 Muzio M, Chinnaiyan AM, Kischkel FC *et al.* FLICE, a novel FADD-homologous ICE/CED-3-like protease, is recruited to the CD95 (Fas/APO-1) death–inducing signaling complex. *Cell* 1996; **85**: 817–27.
14 Chaudhary PM, Eby MT, Jasmin A, Kumar A, Liu L, Hood L. Activation of the NF-kappaB pathway by caspase 8 and its homologs. *Oncogene* 2000; **19**: 4451–60.
15 Hu WH, Johnson H, Shu HB. Activation of NF-kappaB by FADD, Casper, and caspase-8. *J Biol Chem* 2000; **275**: 10838–44.
16 Soung YH, Lee JW, Kim SY *et al.* Caspase-8 gene is frequently inactivated by the frameshift somatic mutation 1225_1226delTG in hepatocellular carcinomas. *Oncogene* 2005; **24**: 141–7.
17 Mandruzzato S, Brasseur F, Andry G, Boon T, van der Bruggen P. A CASP-8 mutation recognized by cytolytic T lymphocytes on a human head and neck carcinoma. *J Exp Med* 1997; **186**: 785–93.
18 Kim HS, Lee JW, Soung YH *et al.* Inactivating mutations of caspase-8 gene in colorectal carcinomas. *Gastroenterology* 2003; **125**: 708–15.
19 Soung YH, Lee JW, Kim SY *et al.* CASPASE-8 gene is inactivated by somatic mutations in gastric carcinomas. *Cancer Res* 2005; **65**: 815–21.
20 Eberstadt M, Huang B, Chen Z *et al.* NMR structure and mutagenesis of the FADD (Mort1) death-effector domain. *Nature* 1998; **392**: 941–5.
21 Tibbetts MD, Zheng L, Lenardo MJ. The death effector domain protein family: regulators of cellular homeostasis. *Nat Immunol* 2003; **4**: 404–9.
22 Yu JW, Shi Y. FLIP and the death effector domain family. *Oncogene* 2008; **27**: 6216–27.

23 Budd RC, Yeh WC, Tschopp J. cFLIP regulation of lymphocyte activation and development. *Nat Rev Immunol* 2006; **6**: 196–204.
24 Kischkel FC, Lawrence DA, Tinel A *et al.* Death receptor recruitment of endogenous caspase-10 and apoptosis initiation in the absence of caspase-8. *J Biol Chem* 2001; **276**: 46639–46.
25 Wang J, Chun HJ, Wong W, Spencer DM, Lenardo MJ. Caspase-10 is an initiator caspase in death receptor signaling. *Proc Natl Acad Sci USA* 2001; **98**: 13884–8.
26 Sprick MR, Rieser E, Stahl H, Grosse-Wilde A, Weigand MA, Walczak H. Caspase-10 is recruited to and activated at the native TRAIL and CD95 death-inducing signalling complexes in a FADD-dependent manner but can not functionally substitute caspase-8. *EMBO J* 2002; **21**: 4520–30.
27 Shikama Y, Yamada M, Miyashita T. Caspase-8 and caspase-10 activate NF-kappaB through RIP, NIK and IKKalpha kinases. *Eur J Immunol* 2003; **33**: 1998–2006.
28 Pop C, Fitzgerald P, Green DR, Salvesen GS. Role of proteolysis in caspase-8 activation and stabilization. *Biochemistry* 2007; **46**: 4398–407.
29 Krammer PH. CD95's deadly mission in the immune system. *Nature* 2000; **407**: 789–95.
30 Heyninck K, Beyaert R. Crosstalk between NF-kappaB-activating and apoptosis-inducing proteins of the TNF-receptor complex. *Mol Cell Biol Res Commun* 2001; **4**: 259–65.
31 Varfolomeev E, Maecker H, Sharp D *et al.* Molecular determinants of kinase pathway activation by Apo2 ligand/tumor necrosis factor-related apoptosis-inducing ligand. *J Biol Chem* 2005; **280**: 40599–608.
32 Golks A, Brenner D, Krammer PH, Lavrik IN. The c-FLIP-NH2 terminus (p22-FLIP) induces NF-kappaB activation. *J Exp Med* 2006; **203**: 1295–305.
33 Stransky N, Egloff AM, Tward AD *et al.* The mutational landscape of head and neck squamous cell carcinoma. *Science* 2011; **333**: 1157–60.

Supporting Information

Additional Supporting Information may be found in the online version of this article:

Fig. S1. Non-synonymous mutations in caspase-8. CRC, colorectal cancer; GC, gastric cancer; HCC, hepatocellular carcinoma; HNSCC, head and neck squamous cell carcinoma.

Fig. S2. Caspase-8 (CASP8) affects annexin V-positive fractions in T3M-1 Cl-10 head and neck squamous cell carcinoma cells but not in OE21 esophageal squamous cell carcinoma cells.

Fig. S3. Depletion of *CASP8* message leads to a decrease in *BCL2* expression.

Fig. S4. Structure of human death effector domain (DED) family members.

Table S1. Caspase-8 (CASP8) non-synonymous mutations identified in previously published reports.

doi: 10.1111/cas.12191

THE JOURNAL OF BIOLOGICAL CHEMISTRY VOL. 288, NO. 13, pp. 9457–9467, March 29, 2013

Mutations in the Nucleolar Phosphoprotein, Nucleophosmin, Promote the Expression of the Oncogenic Transcription Factor MEF/ELF4 in Leukemia Cells and Potentiates Transformation*

Received for publication, September 3, 2012, and in revised form, February 5, 2013 Published, JBC Papers in Press, February 7, 2013, DOI 10.1074/jbc.M112.415703

Koji Ando[‡], Hideki Tsushima[§], Emi Matsuo[¶], Kensuke Horio[‖], Shinya Tominaga-Sato[**], Daisuke Imanishi[‡], Yoshitaka Imaizumi[§], Masako Iwanaga[‡], Hidehiro Itonaga[‡], Shinichiro Yoshida[¶], Tomoko Hata[§], Ryozo Moriuchi[‡‡], Hitoshi Kiyoi[§§], Stephen Nimer[¶¶], Hiroyuki Mano[‖‖], Tomoki Naoe[§§], Masao Tomonaga[‖], and Yasushi Miyazaki[‡1]

From the [‡]Department of Hematology, Atomic Bomb Disease and Hibakusha Medicine Unit, Nagasaki University Graduate School of Biomedical Sciences, 1-12-4 Sakamoto, Nagasaki, Nagasaki 852-8523, Japan, the [§]Department of Hematology, Nagasaki University Hospital, Nagasaki, Nagasaki 852-8523, Japan, the [¶]Department of Hematology, Nagasaki Medical Center, Omura, Nagasaki 856-0835, Japan, the [‖]Department of Hematology, Japanese Red-Cross Nagasaki Atomic Bomb Hospital, Nagasaki, Nagasaki 852-8104, Japan, the [**]Division of Hematology, Sasebo City General Hospital, Sasebo, Nagasaki 857-8511, Japan, the [‡‡]Department of Internal Medicine, Keijyu Hospital, Isahaya, Nagasaki 854-0121, Japan, the [§§]Department of Hematology and Oncology, Nagoya University Graduate School of Medicine, Nagoya 466-8550, Japan, the [¶¶]Sloan-Kettering Institute, Memorial Sloan-Kettering Cancer Center, New York, New York 10021, and the [‖‖]Division of Functional Genomics, Jichi Medical University, Shimotsuke, Tochigi 329-0498, Japan

Background: MEF/ELF4 can function as an oncogene. We demonstrated the role of MEF/ELF4 in acute myeloid leukemia.
Results: NPM1 inhibited the DNA binding and transcriptional activity of MEF/ELF4 on the HDM2 promoter, whereas NPM1 mutant protein enhanced these activities of MEF/ELF4.
Conclusion: MEF/ELF4 activity may be activated by NPM1 mutant protein.
Significance: NPM1 mutant proteins have a role in MEF/ELF4-dependent leukemogenesis.

Myeloid ELF1-like factor (MEF/ELF4), a member of the ETS transcription factors, can function as an oncogene in murine cancer models and is overexpressed in various human cancers. Here, we report a mechanism by which MEF/ELF4 may be activated by a common leukemia-associated mutation in the nucleophosmin gene. By using a tandem affinity purification assay, we found that MEF/ELF4 interacts with multifactorial protein nucleophosmin (NPM1). Coimmunoprecipitation and GST pull-down experiments demonstrated that MEF/ELF4 directly forms a complex with NPM1 and also identified the region of NPM1 that is responsible for this interaction. Functional analyses showed that wild-type NPM1 inhibited the DNA binding and transcriptional activity of MEF/ELF4 on the HDM2 promoter, whereas NPM1 mutant protein (Mt-NPM1) enhanced these activities of MEF/ELF4. Induction of Mt-NPM1 into MEF/ELF4-overexpressing NIH3T3 cells facilitated malignant transformation. In addition, clinical leukemia samples with NPM1 mutations had higher human MDM2 (HDM2) mRNA expression. Our data suggest that enhanced HDM2 expression induced by mutant NPM1 may have a role in MEF/ELF4-dependent leukemogenesis.

Myeloid ELF1-like factor (MEF/ELF4), a member of the ETS family of transcription factors, is characterized by an 85-amino acid ETS domain that recognizes a core sequence of GGAA or TTCC (1). MEF/ELF4 is expressed in various normal and malignant hematopoietic cells and regulates the expression of various cytokines (interleukin-3 (1), granulocyte-macrophage colony-stimulating factor (1), and interleukin-8 (2) as well as the cytolytic perforin molecule (3) and antibacterial peptides lysozyome and human β-defensin2 (4)) and matrix metalloproteinase-9 expression (5). Furthermore, analyses of MEF/ELF4-deficient mice have revealed the essential role of MEF/ELF4 in the development and function of NK (natural killer) cells and NK-T cells (3). Recently, Smith *et al.* (6) have shown that repression of Elf-4 by transcriptional repressor *Gfi1b* is important for the maturation of primary fetal liver erythroid cells. MEF/ELF4 also regulates the key aspects of hematopoietic stem cell behavior by controlling movement through the cell cycle from quiescence (G_0) to G_1 and from G_1 to S as well as resistance to myelosuppression (7, 8).

MEF/ELF4 is expressed in cancers such as leukemia (9), lymphoma, and ovarian cancer (10). Recently, Totoki *et al.* (11) identified an intrachromosomal inversion (Xq25) in hepatocellular carcinoma that generated a BCORL1-MEF/ELF4 fusion transcript. Experiments in several mouse models have suggested that MEF/ELF4 plays a role in tumorigenesis. For example, models of retrovirus-induced insertional mutagenesis have identified *MEF/ELF4* as a gene that is involved in leukemic transformation (12). Sashida *et al.* (13) have shown that overexpression of MEF/ELF4 enhances the expression of Mdm2,

* This work was supported in part by a grant from the Ministry of Health, Welfare, and Labor and a grant from the Ministry of Education, Culture, Sports, Science, and Technology of Japan.
[1] To whom correspondence should be addressed. Tel.: 81-95-819-7111; Fax: 81-95-819-7113; E-mail: y-miyaza@nagasaki-u.ac.jp.

leading to decreased p53 expression and enhanced transformation. In experiments with MEF/ELF4-overexpressing cells, they demonstrated that Ets1-induced p16 induction is suppressed, resulting in senescence suppression and tumor promotion.

Nucleophosmin (NPM1) is a nucleolar phosphoprotein (14) and a frequent target of genetic alterations in hematopoietic malignancies. *NPM1* gene mutations have been found in ~60% of adult patients who have acute myeloid leukemia (AML)[2] and a normal karyotype (15). These mutations lead to the aberrant cytoplasmic expression of NPM1 ($NPMc^+$) due to nucleotide gain at the C terminus (16, 17), which results in the loss of tryptophan residues essential for nucleolar localization and the gain of a new nuclear export signal (18). Increased NPM1 export into the cytoplasm probably perturbs multiple cellular pathways by delocalizing the proteins that interact with NPM1. By using a transgenic mouse model expressing the human $NPMc^+$ mutation, it has been shown that $NPMc^+$ confers a proliferative advantage in the myeloid lineage, suggesting that NPM1 mutations can participate in leukemia development (19).

In the present study, we found that wild-type NPM1 (Wt-NPM1) down-regulates, whereas mutated NPM1 (Mt-NPM1) up-regulates, the transcriptional activity of MEF/ELF4 on the human MDM2 (HDM2) promoter. The expression of Mt-NPM1 in MEF/ELF4-overexpressing NIH3T3 cells resulted in enhanced malignant transformation. We also found that *HDM2* mRNA expression in primary AML cells with *NPM1* mutations is significantly higher compared with AML cells without *NPM1* mutations. Taken together, our data suggest that *NPM1* mutations may promote transformation by enhancing the oncogenic functions of MEF/ELF4.

EXPERIMENTAL PROCEDURES

Cell Culture—293T cells (CRL-11268, ATCC (Manassas, VA)) were maintained at 37 °C in DMEM (Invitrogen) with bovine calf serum. U937 cells (CRL-1593.2, ATCC) were maintained with 10% (v/v) FBS, 100 IU/ml penicillin, and 100 μg/ml streptomycin (Fisher). NIH3T3 cells (CRL-1658, ATCC) were maintained under identical conditions with 10% (*v/v*) FBS and grown in RPMI 1640 (Fisher) with 10% FCS (HyClone, Logan, UT), 100 units/ml penicillin G, and 100 μg/ml streptomycin. COS7 cells (CRL-1651, ATCC) were cultured in DMEM (Invitrogen) containing 10% FCS.

Tandem Affinity Purification Assay—The cDNA of MEF/ELF4 was inserted into InterPlay N-terminal mammalian TAP vector (pTAP/MEF/ELF4, Stratagene (San Diego, CA)) comprising two affinity tags (immunoglobulin G (IgG)-binding domain and calmodulin-binding peptide) separated by the cleavage site of tobacco etch virus protease (20). 293T cells were transfected with pTAP or pTAP/MEF/ELF4 plasmids in a 10-cm dish. Transfected cells were collected and lysed in a solution containing 100 mM Tris-HCl (pH 8.0), 300 mM NaCl, and 0.1% Nonidet P-40. The lysate was centrifuged at 15,000 rpm for 30 min at 4 °C. The resulting supernatant was incubated for 2 h at 4 °C with IgG-Sepharose 6 Fast Flow (GE Healthcare), after which the resin was washed and incubated with tobacco etch virus protease for 2 h at 16 °C. Purification on calmodulin affinity resin (Stratagene) was performed according to the manufacturer's instructions. Purified proteins were precipitated with trichloroacetic acid, resolved with 1× sample buffer and subjected to SDS-PAGE. Gels were stained with Coomassie Blue, and protein bands were cut out. Proteins were eluted with trypsin. The resulting peptides were analyzed with a Procise 49X cLC protein sequencer (Applied Biosystems, Foster City, CA) (20).

In Vitro Translation—The cDNA molecules of Wt-NPM1 and Mt-NPM1 (21) were inserted into the pTnT vector (pTnT-NPM, Promega (Madison, WI)) for *in vitro* translation. NPM1 protein (biotin-NPM1) was *in vitro*-translated with pTnT-NPM1 and labeled with biotinylated lysine (Transcend tRNA, Promega) by using the TNT Quick Coupled transcription/translation system (Promega). The cDNA of MEF/ELF4 was inserted into pET-3a (Novagen, VWR (Lisbon, Portugal)), which allows the introduction of a His tag into the N terminus of MEF/ELF4 (pET/MEF/ELF4). Overexpression of the recombinant protein (His-MEF/ELF4) was achieved in *Escherichia coli* BL21Gold (DE3) cells (Stratagene) transformed with the constructed plasmid pET/MEF/ELF4. His-MEF/ELF4 was isolated from cells broken in lysis buffer (STE buffer) with sonication and centrifuged at 15,000 × *g* for 10 min at 4 °C (1).

Biotin-NPM1 was incubated with His-MEF/ELF4 or His (as a control) proteins at 4 °C for 1 h. The mixture was loaded onto His spin traps (GE Healthcare) and eluted with 500 mM imidazole at pH 7.4. After SDS-PAGE and electroblotting, biotin-NPM1 in purified samples was detected by using the Transcend non-radioactive translation detection system (Promega).

Immunoprecipitation and Immunoblotting—MEF/ELF4 was cloned into p3xFLAG-CMV (Sigma) (FLAG-MEF/ELF4) from PCR products generated from pcDNA/MEF/ELF4 (1). Wt-NPM1 and Mt-A-NPM1 were cloned into pcDNA3.1/V5-His (pcDNA/V-Wt-NPM1 and Mt-A-NPM1, respectively) (Invitrogen) from PCR products generated from pcDNA/Wt-NPM1 and pcDNA/Mt-A (21). 293T cells were transfected with each plasmid by using Effectene transfection reagent (Qiagen, Berlin, Germany). After 48 h, cells were lysed by using the Universal Magnetic co-immunoprecipitation kit (Active Motif, Carlsbad, CA) following the manufacturer's instructions for nuclear extraction. Lysates were centrifuged at 15,000 rpm for 10 min at 4 °C to remove the resin. The resulting supernatants were incubated for 4 h at 4 °C with 5 μg of antibodies against FLAG (Sigma), 5 μg of antibodies against V5 (Invitrogen), or normal mouse IgG (Santa Cruz Biotechnology, Inc., Santa Cruz, CA).

Immunoprecipitates were recovered, washed four times with ice-cold co-immunoprecipitation solution (Active Motif), and fractionated by SDS-PAGE. Separated proteins were transferred to a membrane. After incubation in blocking buffer, membranes were probed with peroxidase-labeled antibodies against FLAG (Sigma), V5 (Invitrogen), or tag (Invitrogen). Detection was achieved with an enhanced chemiluminescence system (ECL Advance Western blotting detection kit, GE Healthcare). Quantification of Western blotting bands was per-

[2] The abbreviations used are: AML, acute myeloid leukemia; Wt-NPM1, wild type NPM1; Mt-NPM1, mutant NPM1; RQ-PCR, quantitative reverse transcription-polymerase chain reaction.

formed by using AE-6982/C/FC and CS Analyzer version 3.0 software (ATTO, Tokyo, Japan).

GST and His Pull-down Assay—Fusion protein of GST and Wt-NPM1 (GST-NPM1) and GST-NPM1 deletion mutant constructs (Fig. 1*C*) were generated by PCR with pcDNA/Wt-NPM1 as a template. PCR products were cloned in-frame into bacterial expression vector pGEX-T4. Plasmids that express GST fusion protein (GST-NPM1, GST-NPM1 deletion mutants) and His-MEF/ELF4 protein (pET/MEF/ELF4) or their controls were transfected into *E. coli*. Bacterial pellets were lysed in 1 ml of phosphate-buffered saline (PBS) with sonication. His-MEF/ELF4 or His alone was incubated with an equivalent amount of GST, GST-Wt-NPM1, or GST-Wt-NPM1 deletion mutants for 1 h at 4 °C. Proteins were purified by using GST columns (MicroSpin GST Purification Module, GE Healthcare) or His columns. Bound proteins were analyzed by using SDS-PAGE/immunoblot.

EMSA—Recombinant proteins GST, GST-NPM1, His, and His-MEF/ELF4 were collected as described above. Nuclear protein from 293T cells transfected with pcDNA/MEF/ELF4, pcDNA/Wt-NPM1, or pcDNA/Mt-A-NPM1 was extracted with the NE-PER nuclear and cytoplasmic extraction kit (Pierce) according to the manufacturer's instructions. EMSA was performed by using the LightShift chemiluminescent EMSA kit (Pierce). Recombinant protein or nuclear extracts were incubated with 20 fmol of biotin 3′-end-labeled oligonucleotides containing APET (an ETS binding site in the IL-3 promoter that was shown to bind to MEF/ELF4) (1). After electrophoresis, transfer, and cross-linking, the signal was detected by a peroxidase/luminol system (chemiluminescent nucleic acid detection module, Pierce). To confirm specificity, a 200-fold excess amount of non-labeled oligonucleotides (APET competitor) (1) was added. The DNA sequence of the APET oligonucleotide is 5′-CCTCAGTGAGCTGAGTCAGG-CTTCCCCTTCCTGCCACAGGG-3′.

RNA Interference—siRNA for NPM1 was transfected into 293T cells by using the GeneClip U1 hairpin cloning system (Promega) according to the manufacturer's instructions. The siRNA sequence-targeting NPM1 gene corresponded to nucleotides 103–125 of the coding region relative to the first nucleotide of the start codon, as described previously (22).

Luciferase Assay—A 0.5-μg aliquot of pcDNA/MEF/ELF4, pcDNA/Wt-NPM1, pcDNA/Mt-A-NPM1, pcDNA/Mt-I-NPM1, or pcDNA/Mt-J-NPM1 was transfected into U937, 293T, and COS7 cells seeded in 6-well dishes by using Nucleofectin (Qiagen) together with 0.1 μg of pGL4 reporter plasmid (pGL4/APET (1), pGL4/ETSm-APET (1), pGL4/HDM2, or pGL4/HDM2mut) and 0.05 μg of pLR-Bact vector. pGL4/ETSm-APET contains a mutation in the ETS binding site (ETSm-APET, 5′-CCTCAGTGAGCTGAGTCAGGCTgagC-CTcgacGCCACAGGG-3′). pGL4/HDM2 contains a wild-type hdm2 (P2) promoter sequence from bp −82 to −122 (Wt-Ets, CAGGTTGACTCAGCTTTTCCTCTTGAGCTGGTCAAG-TTCAG), and pGL4/HDM2mut contains an hdm2 (P2) promoter sequence with a mutated ETS site (Mt-Ets, CAGGTTG-ACTCAGCTTTTaCTCTTGAGCTGGTCAAGTTCAG) (23). Cell lysates were prepared 48 h after transfection, and luciferase activity was determined by using the Dual-Luciferase reporter assay system (Promega).

Anchorage-independent Growth Assay—NIH3T3 cells were plated on 24-well dishes in soft agar containing DMEM supplemented with 10% FCS after they were transfected with various combinations of empty vector, pcDNA/MEF/ELF4, pcDNA/Wt-NPM1, or pcDNA/Mt-A-NPM1 and cultured for 2 weeks. Images were taken with a Leica DM IRBE inverted microscope (Leica Microsystems GmbH, Mannheim, Germany) with a ×10 objective lens.

Immunochemistry—MEF/ELF4 was cloned into the pGFP-C3 vector (Clontech, Mountain View, CA) (pGFP-MEF/ELF4). 293T cells were transfected with the empty vector, pGFP-MEF/ELF4, pcDNA/V-Wt-NPM1, or pcDNA/V-Mt-A-NPM1. Cells were harvested 3 days after transfection. Cytospin samples were fixed for 15 min in PBS containing 4% paraformaldehyde. Fixed coverslips were washed twice in TBS, permeabilized in 0.5% Triton X-100 for 10 min, and incubated in Image-iT FX signal enhancer (Invitrogen) for 30 min. Cells were incubated with primary antibody for 1 h and then washed extensively in TBS before incubation with Alexa546-conjugated goat anti-mouse-IgG antibody (dilution 1:2000; Invitrogen) for 1 h. Cells were covered with a drop of ProLong Gold Antifade Reagent with DAPI (Invitrogen). Fluorescent images were obtained by using a confocal laser-scanning microscope (LSM 5 Pascal V3.2, Carl Zeiss).

ChIP Assay—293T cells were transfected with empty vector, pcDNA/MEF-FLAG, pcDNA/Wt-NPM1, or pcDNA/Mt-A-NPM1 by using a nucleofection kit (Qiagen). After 48 h of culture at 26 °C, cells were fixed by the addition of 1% formaldehyde in PBS for 10 min. Chromatin isolation and shearing were performed by using the OneDay ChIP kit (Diagenode, Liege, Belgium) and Shearing-ChIP kit (Diagenode) according to the manufacturer's instructions. Immunoprecipitation reactions were performed with anti-FLAG monoclonal antibody (Sigma) or isotype control IgG (BD Biosciences). Samples were analyzed by quantitative reverse transcription-polymerase chain reaction (RQ-PCR) by using the LightCycler DNA Master SYBR Green I kit (Roche Applied Science) as specified by the manufacturer. The primer sequences for the HDM2 promoter were 5′-GAACGCTGCGCGTAGTCTGG-3′ (forward) and 5′-ACTGC-AGTTTCGGAACGTGT-3′ (reverse).

Clinical Samples—Informed consent for sample collection was obtained according to protocols approved by the International Review Board of Nagasaki University, Nagasaki, Japan (approval number 33-3). Bone marrow aspirates were collected from 22 AML patients before the initiation of chemotherapy. CD34-positive cells were isolated by using Ficoll density gradient centrifugation and magnetic beads (CD34 Isolation Kit, Miltenyi Biotec, Auburn, CA) to minimize the confounding effect of MEF/ELF4 and NPM1 expression by mature myeloid cells. For the screening of *NPM1* mutations, genomic DNA corresponding to exon 12 was amplified by using forward primer 5′-TTAACTCTCTGGTGGTAGAATGAA-3′ and reverse primer 5′-CAAGACTATTTGCCATTCCTAAC-3′, as reported previously. Amplified products were separated by agarose gel electrophoresis, purified by using a QIAquick gel extraction kit (Qiagen), and directly sequenced by using a DNA sequencer

(3100, Applied Biosystems) with the BigDye terminator cycle sequencing kit (Applied Biosystems). When mutations were found by direct sequencing, the fragments were cloned into a pTOPO vector (Invitrogen) and then transfected into the *E. coli* strain DH5A. At least four recombinant colonies were selected, and plasmid DNA samples were prepared by using the QIAprep Spin Miniprep kit (Qiagen). Cloned fragments were sequenced to confirm the mutation of the *NPM1* gene.

Total RNA was harvested from purified CD34-positive cells by using an RNeasy minikit (Qiagen). cDNA synthesis was undertaken by using an oligo(dT) primer with the PrimeScript II first strand cDNA synthesis kit (Takara, Shiga, Japan). These cDNA molecules were measured by RQ-PCR with the primers listed under "RQ-PCR."

RQ-PCR—RQ-PCR was performed by using a LightCycler TaqMan Master kit (Roche Applied Science) following the manufacturer's instructions. Twenty microliters of Universal ProbeLibrary probes (Exiqon, Vedbaek, Denmark) were added in the final reaction. Primers designed by using the Universal ProbeLibrary Assay Design Centre (available on the Roche Applied Science Web site) were synthesized by Sigma. PCR amplification was performed by using a LightCycler 350S instrument (Roche Applied Science). Thermal cycling conditions comprised 2 min at 40 °C and 10 min at 95 °C, followed by 45 amplification cycles at 95 °C for 10 s, 60 °C for 30 s, and 72 °C for 1 s and then a 40 °C cooling cycle for 30 s. Specific primers and probes were as follows: for *HDM2*, forward (5′-TCTGATAGTATTTCCCTTTCCTTTG-3′), reverse (5′-TGTTCACTTACACCAGCATCAA-3′), and probe (5′-CGCCACTTTTTCTCTGCTGATCCAGG-3′); for human *MEF/ELF4*, forward (5′-TGGAGACTCTCAGGGTCGAAA-3′), reverse (5′-AAGCAACGGGATGGATGAT-3′), and probe (5′-TCACAGCTGGGAACACAGAG-3′); and for human *G6PDH*, forward (5′-AAGCAACGGGATGGATGAT-3′), reverse (5′-TCACAGCTGGGAACACAGAG-3′), and probe (5′-CGCCACTTTTTCTCTGCTGATCCAGG-3′).

Statistical Analyses—Comparisons of patient characteristics between two groups were performed with the Wilcoxon test. The results of *in vivo* experiments are presented as the mean ± S.D. of three independent experiments and compared by using one-way analysis of variance followed by Scheffe's multiple comparison test. A p value of 0.05 was considered statistically significant.

RESULTS

Identification of MEF/ELF4-binding Protein—To identify the proteins that bind to MEF/ELF4, we performed the tandem affinity purification (TAP) procedure and analyzed the amino acid sequence of the protein complex, thereby identifying 25 proteins (including NPM1). NPM1 is essential for embryonic development and is frequently translocated or mutated in hematological malignancies (24). Therefore, we decided to focus on the interaction between NPM1 and MEF/ELF4.

Wt-NPM1 Interacts with MEF/ELF4 in Vivo and in Vitro—To determine if Wt-NPM1 interacts with MEF/ELF4 in human cells, we transfected 293T cells with FLAG-MEF/ELF4 and V5-Wt-NPM1 expression plasmids and performed immunoprecipitations with mouse monoclonal anti-FLAG or anti-V5 antibody. As shown in Fig. 1*A*, FLAG-MEF/ELF4 protein co-precipitated with V5-Wt-NPM1 by the anti-V5 antibody (*lane 1*) but not by the isotype-matched control (*lane 2*). In reciprocal experiments, V5-Wt-NPM1 protein co-precipitated with FLAG-MEF/ELF4 protein by the anti-FLAG antibody (*lane 3*). These results showed the *in vivo* interaction between Wt-NPM1 and MEF/ELF4. To ascertain whether Wt-NPM1 protein interacted directly with MEF/ELF4, an *in vitro* association assay with biotin-labeled *in vitro*-translated Wt-NPM1 and bacterially recombinant His-MEF/ELF4 fusion protein was performed (Fig. 1*B*). Biotin-labeled Wt-NPM1 bound to His-MEF/ELF4 (*lane 1*) but not to His alone (*lane 2*). These results demonstrated that His-MEF/ELF4 bound directly to Wt-NPM1.

To characterize the region of Wt-NPM1 that binds MEF/ELF4, five distinct GST-NPM1 proteins were prepared (Fig. 1*C*). GST pull-down assays (Fig. 1*D* (*a*)) and His tag pull-down assays (Fig. 1*D* (*b*)) revealed that the N-terminal region of NPM1 (the F1, F2, and F3 fragments that contain the oligomerization domain) bound to His-MEF/ELF4, unlike the C-terminal region of NPM1 (F4 and F5).

Wt-NPM1 Interferes with MEF/ELF4 Binding to Target DNA Sequences—To assess the direct role of Wt-NPM1 in MEF/ELF4 action, we undertook EMSA. His-MEF/ELF4 bound to the APET probe (1), but no band was observed with His, GST, or GST-NPM1 (Fig. 2). The shifted band of MEF/ELF4 was diminished when the APET competitor was added to the reaction mixture. When Wt-NPM1 was added to the reaction mixture, the shifted band containing MEF/ELF4 was diminished. These results implied that Wt-NPM1 inhibits the DNA binding of MEF/ELF4 DNA through direct interactions.

Wt-NPM1 Inhibits, whereas Mt-NPM1 Enhances, MEF/ELF4-dependent Transcriptional Activity—To study the functional relevance of the physical interaction between MEF/ELF4 and Wt-NPM1, we transfected pcDNA/MEF/ELF4 in combination with pcDNA/Wt-NPM1 and examined the activity of the APET promoter construct (1) in 293T cells (Fig. 3*A*). As reported previously, MEF/ELF4 activated the APET promoter by ~159-fold. Co-expression of Wt-NPM1 with MEF/ELF4 led to a significant decrease in luciferase activity. Similar data were obtained by using COS7 cells (Fig. 3*B*) and a human leukemia cell line, U937 (Fig. 3*C*).

Having shown that NPM1 expression attenuated the transcriptional activity of MEF/ELF4 in leukemia cells, we next assessed whether the inhibition of Wt-NPM1 expression *in vivo* enhanced MEF/ELF4-dependent transcriptional activity. The siRNA directed against Wt-NPM1 in 293T cells suppressed the expression of Wt-NPM1 protein by 60–70% (Fig. 3*D*). Transient transfections were performed by using NPM1-knockdown 293T cells with pcDNA/MEF/ELF4 and pGL4/APET reporter plasmids. A luciferase assay revealed that MEF/ELF4-dependent transcriptional activity was significantly elevated in Wt-NPM1-knockdown cells by 1.8-fold (Fig. 3*E*). These results implied that Wt-NPM1 functioned as an inhibitor of MEF/ELF4.

Mutated nucleophosmin (Mt-NPM1) has been found in 50% of adult AML patients with normal karyotypes (15). It has been suggested that the mutation is a critical event for leukemogen-

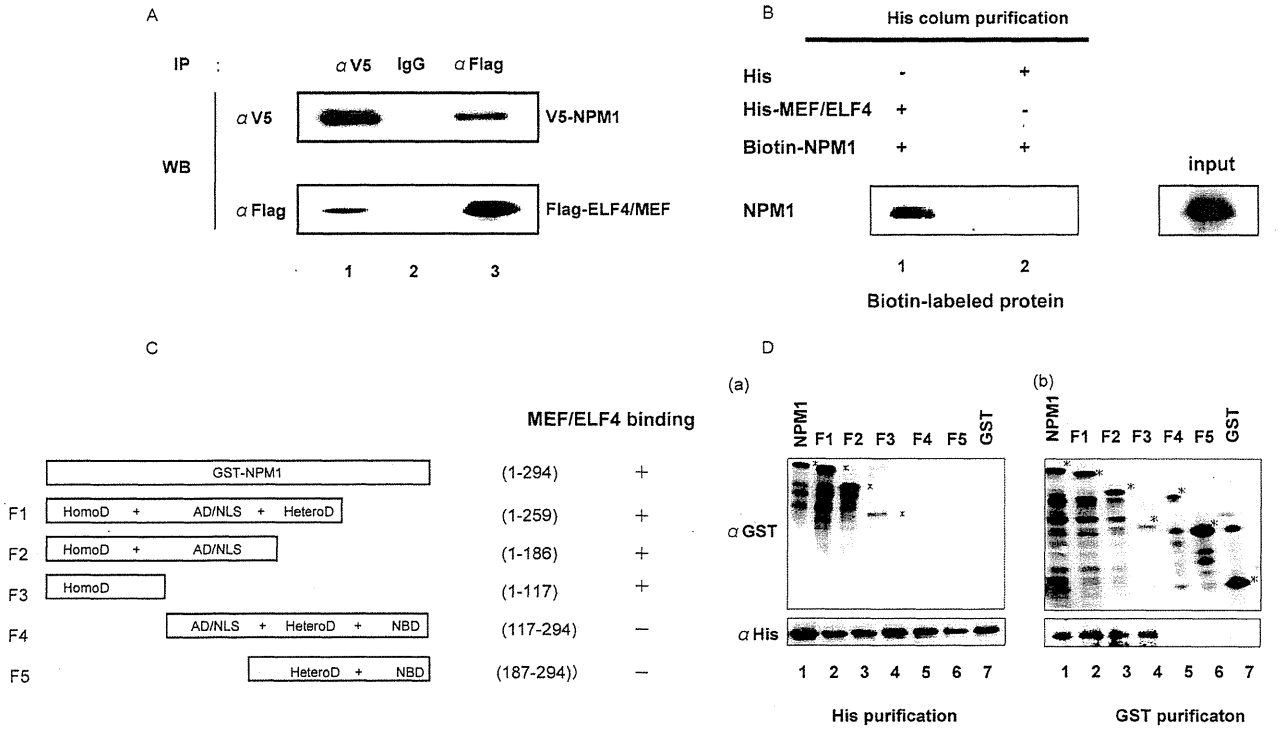

FIGURE 1. **NPM1 interacts with MEF/ELF4.** *A*, 293T cells were transfected with the indicated expression plasmids. After 48 h, cell lysates were immunoprecipitated (*IP*) with anti-FLAG and anti-V5 antibodies. Immunoprecipitates were analyzed by 10% SDS-PAGE and subjected to immunoblotting (*WB*) with anti-V5 antibody (*top row*) or anti-FLAG antibody (*bottom row*). *B*, MEF/ELF4 interacts directly with NPM1 *in vitro*. *In vitro* association assays were undertaken by incubating His-MEF/ELF4 fusion protein immobilized by using a His-column with biotin-labeled MEF/ELF4 (*lane 1*). His alone was incubated with biotin-labeled NPM1 (*lane 2*) as a control. *C*, NPM1 structure and the relative binding of MEF/ELF4 (*schematic*). *HomoD*, homodimerization domain, residues 1–117; *AD/NLS*, acidic domain/nuclear localization sequence, residues 117–187; *HeteroD*, heterodimerization domain, residues 187–259; *NBD*, nucleic acid binding domain, residues 259–294. *D*, the N-terminal portion of NPM1 is the MEF/ELF4-interacting domain. Bacterially expressed and purified GST, GST-NPM1, and GST-NPM1 mutants with deletions were mixed with bacterially expressed and purified His or His-MEF/ELF4 protein. Recombinant proteins were subjected to His or GST affinity columns, followed by immunoblotting with anti-GST or anti-His antibodies. *a*, the reactive samples were subjected to analyses on a His affinity column followed by immunoblotting with anti-His antibodies (*bottom left*) or with anti-GST antibodies (*top left*). *b*, the reactive samples were subjected to GST affinity columns, followed by immunoblotting with anti-GST antibodies (*top right*) or with anti-His antibodies (*bottom right*).

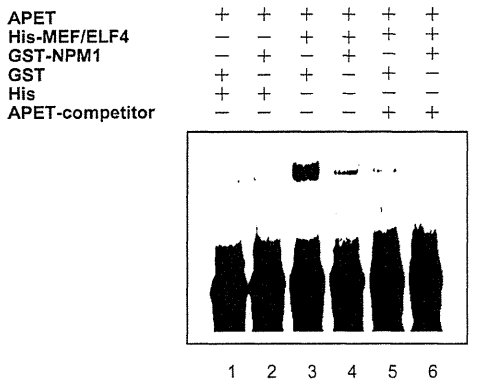

FIGURE 2. **EMSA with recombinant His-MEF/ELF4, His, GST, and GST-Wt-NPM1.** His-MEF/ELF4 was incubated with GST and GST-Wt-NPM1 at room temperature prior to EMSA by using a biotin-conjugated APET probe (*lanes 1–4*). An excess amount of unlabeled APET competitor was added to the reaction mixtures (*lanes 5* and *6*).

esis. To determine the effect of Mt-NPM1 on the transcription-activating properties of MEF/ELF4, we transfected pcDNA/MEF/ELF4 in combination with pcDNA/Mt-A-NPM1, pcDNA/Mt-I-NPM1, or pcDNA/Mt-J-NPM1 and then examined the activity of the APET promoter construct in 293T cells (Fig. 3*F*). Co-expression of Mt-NPM1 with MEF/ELF4 led to a 315-fold increase in luciferase activity. Similar data were obtained with COS7 (Fig. 3*G*) and U937 (Fig. 3*H*) cells. To show the effect of the coexistence of both Wt- and Mt-NPM1, we transfected 293T cells with various amounts of plasmids that expressed Wt-NPM1 and Mt-A-NPM1. The expression of Mt-NPM1 enhanced MEF/ELF4-dependent APET promoter activation in a dose-dependent manner, even in the presence of Wt-NPM1 (Fig. 3*I*). Taken together, our results suggest that Wt-NPM1 has an inhibitory effect, whereas Mt-NPM1 has enhancing effect, on the function of MEF/ELF4.

Mt-NPM1 Does Not Interact with MEF/ELF4 in Vivo—Because the mutated region of Mt-NPM1 was located outside the domain responsible for interaction with MEF/ELF4, we hypothesized that Mt-NPM1 might bind to MEF/ELF4. To test this hypothesis, we transfected 293T cells with FLAG-MEF/ELF4 and V5-Mt-A-NPM1 expression plasmids and performed immunoprecipitations with mouse monoclonal anti-FLAG or anti-V5 antibody. Contrary to our expectations, as shown in Fig. 4, FLAG-MEF/ELF4 protein and V5-Wt-A-NPM1 did not co-precipitate with each other (Fig. 4). These results showed that there is little *in vivo* interaction between Mt-A-NPM1 and MEF/ELF4.

Localization of MEF/ELF4 Is Unaffected by Mt-NPM1—Having shown that Mt-NPM1 enhances the transcriptional activity of MEF/ELF4, we next assessed whether Mt-NPM1 dislocates

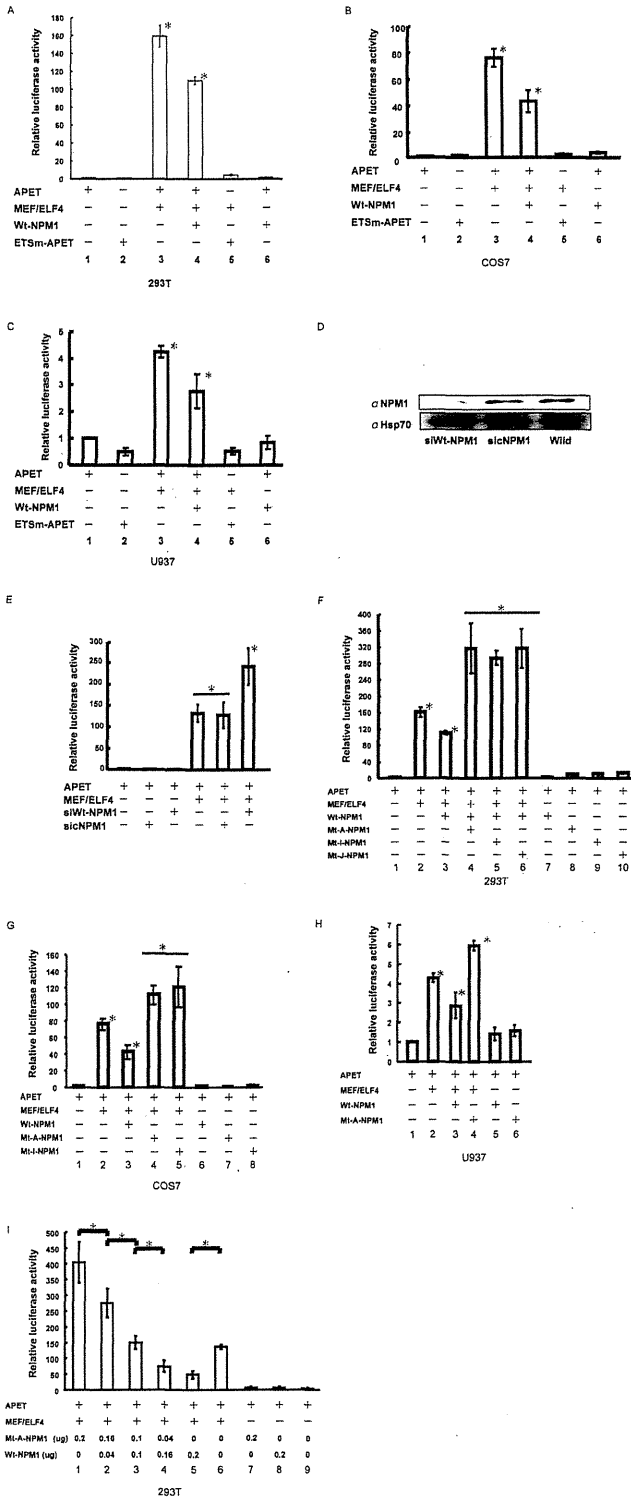

FIGURE 3. **Wt-NPM1 inhibits, whereas Mt-NPM1 enhances, MEF/ELF4-dependent APET promoter transactivation.** 293T human kidney (*A*), COS7 monkey kidney (*B*), and U937 human hematological (C) cell lines were co-transfected with the luciferase reporter gene of an artificial MEF/ELF4 target promoter (APET) and effector genes. The target promoter and effector genes were as follows: pGL4/APET (*lane 1*); pGL4/ETSm-APET (*lane 2*); pGL4/APET and pcDNA/MEF/ELF4 (*lane 3*); pGL4/APET, pcDNA/MEF/ELF4, and pcDNA/Wt-NPM1 (*lane 4*); pGL4/ETSm-APET and pcDNA/MEF/ELF4 (*lane 5*); and pGL4/APET and pcDNA/Wt-NPM1 (*lane 6*). Luciferase activity by pGL4/APET alone was assigned a value of 1.0. The analysis was performed in triplicate assays, and the results were reproducible. The results are shown as the mean ± S.D. (*error bars*). *, $p < 0.05$. *D*, 293T cells transduced with siRNA encoding vector (siWt-NPM1) were harvested 72 h after transduction for Western blotting. Hsp90 is shown as a control. *sicNPM1*, control siRNA non-relevant to the expression of NPM1; *Wild*, without transduction. *E*, 293T cells were co-transfected with the luciferase reporter plasmid (pGL4/APET), expression plasmid (pcDNA MEF/ELF4), and siWt-NPM1 gene (pcDNA/siRNA-Wt-NPM1) or control. Luciferase activity by pGL4/APET alone was assigned a value of 1.0. The analysis was performed in triplicate assays, and the results were reproducible. The results are shown as the mean ± S.D. *, $p < 0.05$. *F*, 293T cells were co-transfected with the luciferase reporter gene of an artificial MEF/ELF4 target promoter and effector genes. Target promoter and effector genes were as follows: pGL4/APET (*lane 1*); pGL4/APET and pcDNA/MEF/ELF4 (*lane 2*); pGL4/APET, pcDNA/MEF/ELF4, and Wt-NPM1 (*lane 3*); pGL4/APET, pcDNA/MEF/ELF4, and Mt-A-NPM1, Mt-I-NPM1, or Mt-J-NPM1 (lanes 4–6, respectively); and pGL4/APET and pcDNA/Wt-NPM1, Mt-A-NPM1, Mt-I-NPM1, or Mt-J-NPM1 (lanes 7–10, respectively). Luciferase activity by pGL4/APET alone was assigned a value of 1.0. The analysis was performed in triplicate assays, and the results were reproducible. The results are shown as the mean ± S.D. *, $p < 0.05$. *G*, COS7 cells were co-transfected with the luciferase reporter gene of an artificial MEF/ELF4 target promoter and effector genes. The target promoter and effector genes were as follows: pGL4/APET (*lane 1*); pGL4/APET and pcDNA/MEF/ELF4 (*lane 2*); pGL4/APET, pcDNA/MEF/ELF4, and Wt-NPM1 (*lane 3*); pGL4/APET, pcDNA/MEF/ELF4, and Mt-A-NPM1 or Mt-I-NPM1 (*lanes 4* and *5*, respectively); and pGL4/APET and pcDNA/Wt-NPM1, Mt-A-NPM1, or Mt-I-NPM1 (*lanes 6–8*, respectively). Luciferase activity by pcDNA/APET alone was assigned a value of 1.0. The analysis was performed in triplicate assays, and the results were reproducible. The results are shown as the mean ± S.D. (*, $p < 0.05$). *H*, U937 cells were co-transfected with the luciferase reporter gene of an artificial MEF/ELF4 target promoter and effector genes. Target promoter and effector genes were as follows: pGL4/APET (*lane 1*); pGL4/APET and pcDNA/MEF/ELF4 (*lane 2*); pGL4/APET, pcDNA/MEF/ELF4, and Wt-NPM1 (*lane 3*); pGL4/APET, pcDNA/MEF/ELF4, and Mt-A-NPM1 (*lane 4*); and pGL4/APET and pcDNA/Wt-NPM1 or Mt-A-NPM1 (*lanes 5* and *6*, respectively). Luciferase activity by pcDNA/APET alone was assigned a value of 1.0. The analysis was performed in triplicate assays, and the results were reproducible. The results are shown as the mean ± S.D. *, $p < 0.05$. *I*, 293T cells were co-transfected with 0.1 μg of the luciferase reporter gene of an artificial MEF/ELF4 target promoter (*lanes 1–9*) and 0.1 μg of effector genes (pcDNA/MEF/ELF4) (*lanes 1–6*). The effector genes were as follows: 0.2 μg of Mt-A-NPM1 (*lane 1*); 0.16 μg of Mt-A-NPM1 and 0.04 μg of Wt-NPM1 (*lane 2*); 0.1 μg of Mt-A-NPM1 and 0.1 μg of Wt-NPM1 (*lane 3*); 0.04 μg of Mt-A-NPM1 and 0.16 μg of Wt-NPM1 or 0.2 μg of Wt-NPM1 (*lanes 4 and 5*, respectively); none (*lane 6*); pGL4/APET and 0.2 μg of Mt-A-NPM1 (*lane 7*); pGL4/APET and 0.2 μg of Wt-NPM1 (*lane 8*); and pGL4/APET (*lane 9*). Luciferase activity by pGL4/APET alone was assigned a value of 1.0. The analysis was performed in triplicate assays, and the results were reproducible. The results are shown as the mean ± S.D. *, $p < 0.05$.

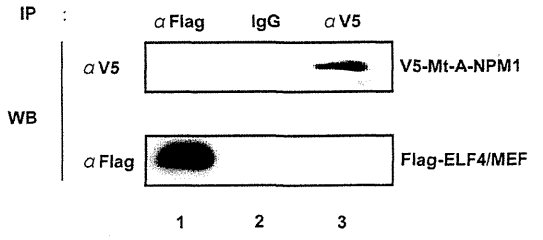

FIGURE 4. **Mt-A-NPM1 does not interact with MEF/ELF4 *in vivo*.** 293T cells were transfected with the indicated expression plasmids. After 48 h, cell lysates were immunoprecipitated (*IP*) with anti-FLAG and anti-V5 antibodies. Immunoprecipitates were analyzed by 10% SDS-PAGE and subjected to immunoblotting (*WB*) with anti-V5 antibody (*top row*) or anti-FLAG antibody (*bottom row*).

MEF/ELF4 into the cytoplasm. We transiently co-transfected a MEF/ELF4-GFP fusion protein vector together with the pcDNA/V-Wt-NPM1 or pcDNA/V-Mt-A-NPM1 expression vector into 293T cells. Wt-NPM1 protein and MEF/ELF4 localized to the nucleus (Fig. 5*A* (*a*)), whereas Mt-A-NPM1 protein localized to the cytoplasm (Fig. 5*A* (b)). Contrary to our expectations, the presence of Mt-A-NPM1 did not affect the subcellular distribution of MEF/ELF4. Western blot analysis of MEF/

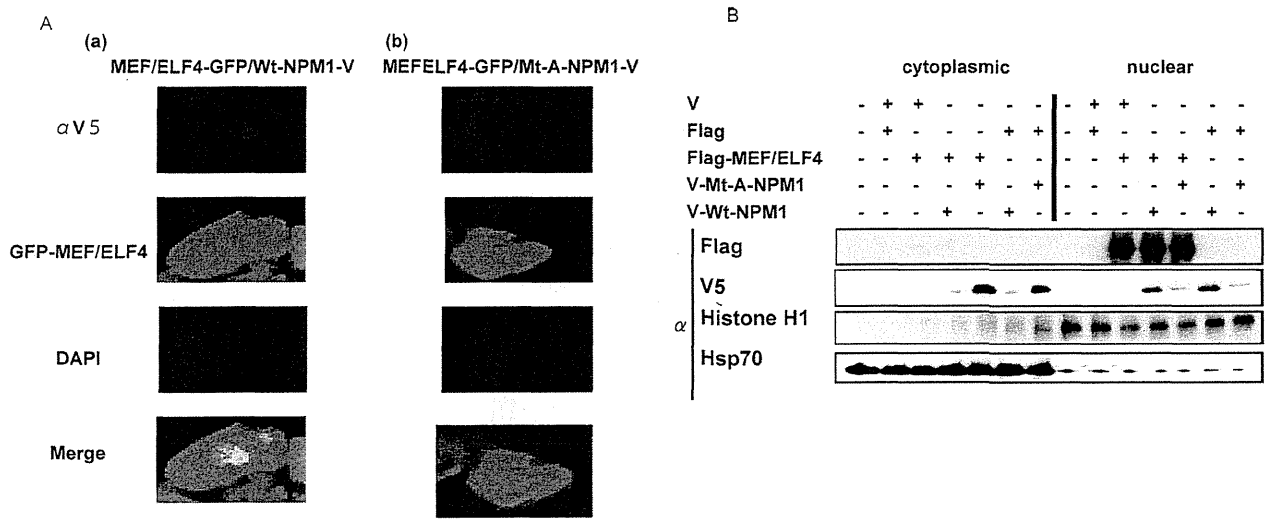

FIGURE 5. **Localization of MEF/ELF4 was unaffected by the mutation of NPM1.** *A*, 293T cells were transfected with the GFP-MEF/ELF4 fusion protein expression vector and pcDNA/V-Wt-NPM1 (*a*) or pcDNA/V-Mt-A-NPM1 (*b*). Forty-eight hours after transfection, cells were fixed and immunofluorescence-stained with anti-V tag antibody. *B*, Western blotting of FLAG-MEF/ELF4 subcellular distribution in 293T cells co-transfected with pFLAG-MEF/ELF4 and pcDNA/V-Wt-NPM1 or pcDNA/V-Mt-A-NPM1. Purity of the subcellular fractions was assessed by blotting with histone H1 (nuclear extraction) and Hsp70 (cytoplasmic extraction).

ELF4 and Wt- or Mt-NPM1 in nuclear and cytoplasmic proteins confirmed the nuclear localization of MEF/ELF4 even with Mt-NPM1 (Fig. 5*B*).

Wt-NPM1 Inhibits, whereas Mt-NPM1 Enhances, the Oncogenic Activity of MEF/ELF4—The overexpression of MEF/ELF4 in NIH3T3 cells increases the growth rate, enhances colony formation in soft agar, and promotes tumor formation in nude mice (10). To determine the effects of the interaction of NPM1 with MEF/ELF4 on cell behavior, we assessed the anchorage-independent growth of NIH3T3 cells after co-transfection of MEF/ELF4 with Wt-NPM1 or Mt-A-NPM1. Compared with NIH3T3 transfected with only MEF/ELF4, Wt-NPM1-coexpressing cells showed reduced anchorage-independent growth, whereas Mt-A-NPM1-coexpressing cells exhibited increased growth (Fig. 6).

MEF/ELF4 Binds to the HDM2 Promoter and Activates Its Expression—In murine cells, MEF/ELF4 binds directly to the Mdm2 promoter, thereby promoting *Mdm2* expression (12). To ascertain whether MEF/ELF4 also directly regulates the promoter activity of *HDM2* (the human analog of Mdm2), we scrutinized the DNA sequence of the *HDM2* gene and found a conserved putative MEF/ELF4 binding site in the P2 promoter (Fig. 7*B*). To establish the association of MEF/ELF4 with the HDM2 promoter, we performed a ChIP assay with nuclear lysates from 293T cells expressing FLAG-MEF/ELF4. Immunoprecipitation with the FLAG antibody (but not with the control IgG) and subsequent PCRs revealed the recruitment of overexpressed MEF/ELF4 to the promoter region of the HDM2 gene (Fig. 7*A*). The luciferase assay revealed that MEF/ELF4 strongly transactivated the wild-type HDM2 promoter (Fig. 7, *B* (*a*) and *C*) and that the effect was abrogated by mutation of the ETS site (−122 to −82) (Fig. 7, *B* (*b*) and *C*). Compared with Wt-NPM1, the expression of Mt-A-NPM1 in 293T cells enhanced the association of MEF/ELF4 with the HDM2 promoter, as detected by ChIP analysis (Fig. 7*D*). Taken together, these findings suggest that Mt-NPM1 up-regulates HDM2 transcription

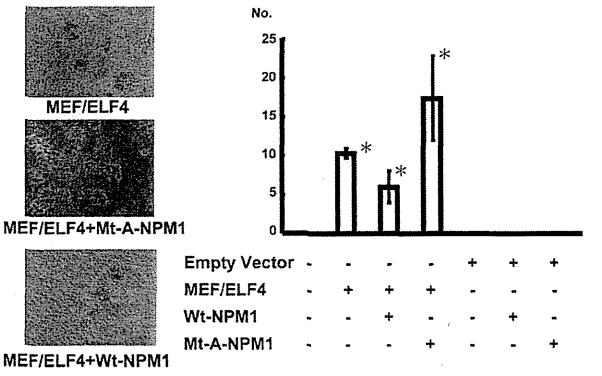

FIGURE 6. **Mt-NPM1 stimulates MEF/ELF4-induced hyperproliferation and transformation.** NIH3T3 cells transfected with various combinations of expression plasmids were plated in soft agar on 60-mm dishes and incubated for 2 weeks. *A*, microscopy of MEF/ELF4-transfected NIH3T3 cells with Wt-NPM1 or Mt-A-NPM1. *B*, the average number of colonies of three independent experiments with S.D. (*error bars*). *, $p < 0.05$.

by increasing the recruitment of MEF/ELF4 to the HDM2 promoter by dislocating Wt-NPM1 that interferes with its binding to the promoter.

Higher Levels of HDM2 mRNA in Clinical Samples from AML Patients with Mt-NPM1 and Higher MEF/ELF4 Expression—To determine the possible clinical relevance of MEF/ELF4, NPM1, and HDM2 in AML patients, we examined the mRNA levels of each in CD34-positive leukemic blasts from 22 AML patients with normal karyotypes. Fourteen patients had Wt-NPM1, and eight patients had Mt-A-NPM1. There was no significant difference between the clinical characteristics of the Wt-NPM1 group and those of the Mt-NPM1 group (Table 1). Samples from the Mt-NPM1 group had significantly higher levels of HDM2 expression as compared with the Wt-NPM1 group ($p = 0.009$) (Fig. 8*A*). In addition, patients with high expression levels of MEF/ELF4 (the MEF/ELF4-H group) had significantly higher HDM2 expression than patients with low expression

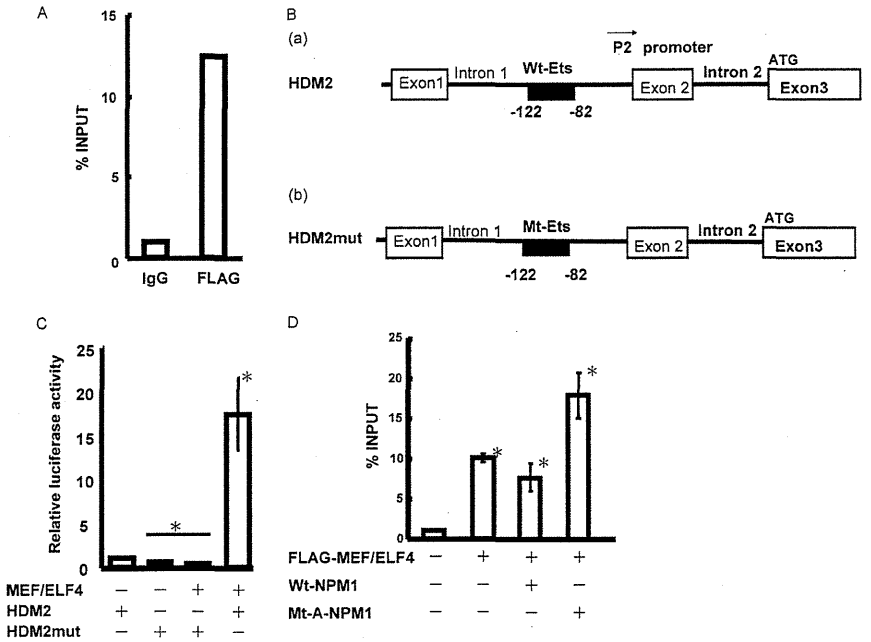

FIGURE 7. **MEF/ELF4 transactivates the HDM2 promoter.** *A*, MEF/ELF4 binds to the HDM2 promoter *in vivo*. FLAG-MEF/ELF4-bound DNA from 293T cells was immunoprecipitated with FLAG antibody or normal mouse IgG. RQ-PCR amplification was performed on the corresponding templates by using primers for HDM2. *B*, structure of the HDM2 promoter region (−82 to −122) (*schematic*). *C*, 293T cells were transfected with HDM2 promoter-driven luciferase reporter plasmid encoding wild-type (*B* (*a*)) or mutant (*B* (*b*)) protein. Luciferase activity by pcDNA alone was assigned a value of 1.0. The analysis was performed in triplicate assays, and the results were reproducible. The results are shown as the mean ± S.D. (*error bars*). *D*, 293T cells were co-transfected with pFLAG/MEF/ELF4 and pcDNA/Wt-NPM1 or pcDNA/Mt-A-NPM1. RQ-PCR amplification was undertaken on corresponding templates using primers for HDM2. The analysis was performed in triplicate assays, and the results were reproducible. The results are shown as the mean ± S.D. *, $p < 0.05$.

TABLE 1
Clinical and laboratory characteristics of patients (ranges shown in parentheses)

	Wt-NPM1	Mt-NPM1	*p*
No. of patients	14	8	
Sex			
Male	5	5	
Female	9	3	0.60
Median age (years)	54.5 (18–78)	62 (44–76)	
FAB classification			
M0	1	0	
M1	2	2	
M2	4	2	
M4	2	2	
M5	2	2	
M6	3	0	0.50
TLD$^+$	6	4	0.50
Median white blood cell count/μl	7300 (1300–556,000)	47,500 (1700–114,700)	0.10
Median lactate dehydrogenase level	647 (203–5325)	669 (270–2391)	0.07
Median bone marrow cell count/μl	337,000 (9000–738,000)	475,000 (34,900–769,000)	0.10

levels of MEF/ELF4 (the MEF/ELF4-L group) ($p = 0.03$) (Fig. 8*B*).

DISCUSSION

In the present study, we identified NPM1 to be a MEF/ELF4-binding protein. Wt-NPM1 inhibited the function of MEF/ELF4 (*i.e.* DNA binding and transcriptional activities), whereas Mt-NPM1 augmented its function. Some of these effects of Wt-NPM1 and Mt-NPM1 on MEF/ELF4 were reproducible on the HDM2 promoter (one of the target genes of MEF/ELF4), suggesting that HDM2 expression is influenced by NPM1. Furthermore, we found that the expression of Mt-NPM1 in MEF/ELF4-overexpressing NIH3T3 cells resulted in enhanced malignant transformation. We also found that the mRNA level of *HDM2* in primary leukemia cells was higher in patients with NPM1 mutations. Mef/Elf4 directly activates *Mdm2* expression (13). Therefore, NPM1 mutation could enhance HDM2 expression through the increased MEF/ELF4 activity, thereby promoting transformation by inhibiting the p53 pathway.

NPM1 is a multifunctional phosphoprotein that has been implicated in cell proliferation as well as regulation of transcription factors. It appears to repress or stimulate transcription. For example, Wt-NPM1 activates and inhibits p53 function through direct binding (22, 25). Interferon regulatory factor-1 (IRF-1), a transcriptional activator, binds to Wt-NPM1, resulting in the inhibition of DNA binding and transcriptional activity (26). Our findings with Wt-NPM1 and MEF/ELF4 are consistent with these observations. Wt-NPM1 interacts directly with c-Myc and regulates the expression of

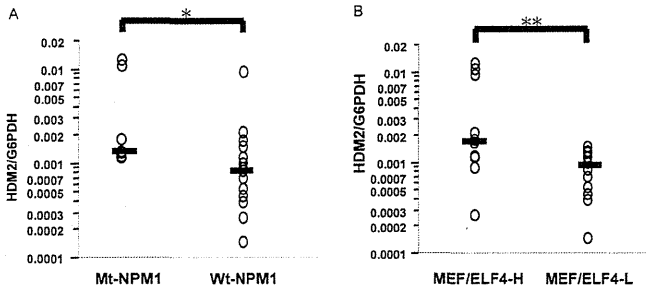

FIGURE 8. **Expression of Mt-NPM1 and higher expression of MEF/ELF4 are associated with the elevated expression of HDM2 in CD34-positive AML cells.** Total RNA isolated from 22 AML patients (CD34-positive leukemia cells) was analyzed for the expression of HDM2 by RQ-PCR. Shown is stratification by the presence of the NPM1 mutation (*A*) and by the level of ELF4/MEF (*B*). These bars were median lines for each group. *, $p < 0.009$ against Wt-NPM1; **, $p < 0.03$ against MEF/ELF4-L, assessed by analysis of variance followed by Scheffe's multiple comparison test.

endogenous c-Myc target genes at the promoter, which enhances c-Myc-induced proliferation and transformation (27). In contrast, the present study suggests that Wt-NPM1 inhibits (whereas Mt-NPM1 facilitates) the transformation induced by MEF/ELF4, suggesting that there is a contradiction in terms of NPM1 function. However, the overexpression of Wt-NPM1 without c-Myc activation has only a small effect on proliferation and has no effect on transformation, so Wt-NPM1 may mainly have a role in c-Myc-driven tumors. Interestingly, c-Myc, IRF-1, and MEF/ELF4 are all regulated during the cell cycle, and the levels of these transcription factors are highest in the G_1 phase (28, 29).

We found that Wt-NPM1 could interfere with the ability of MEF/ELF4 to bind to DNA, resulting in the inhibition of MEF/ELF4-dependent transcriptional activity. The mechanism by which Wt-NPM1 interferes with the DNA binding of MEF/ELF4 is unclear. We previously showed that the 120 amino acids N-terminal to the ETS domain in MEF/ELF4 (residues 87–206) are responsible for its binding to AML1 proteins (30); thus, MEF/ELF4 interacts with other proteins outside the DNA-binding domain. As mentioned above, the association of Wt-NPM1 and IRF-1 inhibits the DNA binding of IRF-1. Narayan *et al.* showed that IRF1 binds directly to Wt-NPM1 through a short linear motif in the nuclear localization sequence outside the DNA-binding domain (31). These results suggest that the inhibition of DNA binding by NPM1 may not be through simple interference with the DNA-binding domain of MEF/ELF4. Determining the protein-binding interface of MEF/ELF4 may help to reveal the mechanism of NPM1-mediated transcriptional regulation.

The heterodimerization domain (residues 186–259) of NPM1 is essential for its interaction with p53 (22), and the c-Myc-binding region is within the NPM1 heterodimerization domain (27). In the case of MEF/ELF4 and NPM1, the N-terminal regions of NPM1 (F1, F2, and F3) could bind to His-MEF/ELF4, implying that the oligomerization domain is important for the interaction.

Recently, it has been shown *in vivo* that NPM1 mutants actively contribute to leukemogenesis by conferring a proliferative advantage in the myeloid lineage. In zebrafish, forced expression of mutant NPM1 causes an increase in PU.1-positive primitive early myeloid cells (32). Furthermore, in a transgenic mouse expressing the human NPM1 mutant, although spontaneous AML was not found, myeloproliferation occurred in the bone marrow and spleen (33). Moreover, Vassiliou *et al.* (34) showed that activation of a humanized mouse NPM1 mutant knock-in allele in mouse hematopoietic stem cells caused overexpression of the *Hox* gene, enhanced self-renewal, and expanded myelopoiesis, resulting in delayed onset AML in one-third of the mice. Taken together, these data suggest that NPM1 mutations initiate leukemia by activating a set of proliferative pathways. Mt-NPM1 enhances the transcriptional activity of MEF/ELF4, so the up-regulation of HDM2 and subsequent down-regulation of p53 may also have a role in leukemogenesis.

In vitro transfection studies and immunohistochemical observations in samples from AML patients have demonstrated that NPM1 mutants recruit Wt-NPM1 from the nucleolus and delocalize it to the nucleoplasm and cytoplasm (18) and that aberrant NPM1 accumulation in the cytoplasm may have a critical role in leukemogenesis. While Wt-NPM1 protein co-localizes with tumor suppressor p19ARF in the nucleolus, Mt-NPM1 delocalizes p19ARF from the nucleolus to the cytoplasm, which results in reduced p19ARF activities (*e.g.* Mdm2 and $p21^{cip1}$ induction, stimulation of NPM1) (35). Furthermore, by using OCI/AML3 human leukemia cells where mutant NPM1 is localized in the cytoplasm, Bhat *et al.* (36) have recently shown that NPM1-co-localizing nuclear transcription factor, FOXM1 (forkhead box M1), disappears from the cytoplasm following transient NPM1 knockdown. These data suggest that NPM1 may determine the intracellular localization of interacting transcription factors. However, in our experiments, Mt-NPM1 did not interact with MEF/ELF4 *in vivo*, and the subcellular distribution of MEF/ELF4 was not affected by the presence of Mt-NPM1. It seems that Mt-NPM1 binds and dislocates Wt-NPM1 into the cytoplasm of leukemia cells, which eventually leads to uncontrolled transactivation of MEF/ELF4. Wt-NPM1 knockdown with siRNA against NPM1 also enhanced MEF/ELF4 activity (Fig. 3*E*), suggesting that the depletion of an MEF/ELF4 inhibitor (*i.e.* Wt-NPM1) in the nucleus is responsible for the transactivation of MEF/ELF4. Taken together, it is likely that NPM1 mutants exert oncogenic functions at least in part through the up-regulation of the activities of oncogenic transcription factors, such as MEF/ELF4. The correlation between NPM1 mutations and the elevated expression of HDM2 in primary leukemia cells seems to support this theory.

In patients with AML, NPM1 mutations are mutually exclusive of recurrent genetic abnormalities. It can be speculated that the enhanced MEF/ELF4-HDM2-p53 pathway induced by NPM1 mutations may participate in leukemia development, especially in patients with a normal karyotype. The transactivation of MEF/ELF4 by E2F1 is inhibited by p53 (37), suggesting that p53 suppression induced by NPM1 mutation could lead to the activation of E2F1, resulting in the enhanced expression of MEF/ELF4. Our previous data showing the elevated expression of MEF/ELF4 in AML cells with a normal karyotype compared with that of AML cells carrying t(8;21) and t(15;17) seem to support this hypothesis.

Our results suggest a new role for NPM1 and MEF/ELF4 in leukemia development.

REFERENCES

1. Miyazaki, Y., Sun, X., Uchida, H., Zhang, J., and Nimer, S. (1996) A novel transcription factor with an Elf-1 like DNA binding domain but distinct transcriptional activating properties. *Oncogene* **13,** 1721–1729
2. Hedvat, C. V., Yao, J., Sokolic, R. A., and Nimer, S. D. (2004) Myeloid ELF1-like factor is a potent activator of interleukin-8 expression in hematopoietic cells. *J. Biol. Chem.* **279,** 6395–6400
3. Lacorazza, H. D., Miyazaki, Y., Di Cristofano, A., Deblasio, A., Hedvat, C., Zhang, J., Cordon-Cardo, C., Mao, S., Pandolfi, P. P., and Nimer, S. D. (2002) The ETS protein MEF plays a critical role in perforin gene expression and the development of natural killer and NK-T cells. *Immunity* **17,** 437–449
4. Lu, Z., Kim, K. A., Suico, M. A., Shuto, T., Li, J. D., and Kai, H. (2004) MEF up-regulates human β-defensin 2 expression in epithelial cells. *FEBS Lett.* **561,** 117–121
5. Seki, Y., Suico, M. A., Uto, A., Hisatsune, A., Shuto, T., Isohama, Y., and Kai, H. (2002) The ETS transcription factor MEF is a candidate tumor suppressor gene on the X chromosome. *Cancer Res.* **62,** 6579–6586
6. Smith, A. M., Calero-Nieto, F. J., Schütte, J., Kinston, S., Timms, R. T., Wilson, N. K., Hannah, R. L., Landry, J. R., Göttgens, B. (2012) Integration of Elf-4 into stem/progenitor and erythroid regulatory networks through locus-wide chromatin studies coupled with *in vivo* functional validation. *Mol. Cell Biol.* **32,** 763–773
7. Lacorazza, H. D., Yamada, T., Liu, Y., Miyata, Y., Sivina, M., Nunes, J., and Nimer, S. D. (2006) The transcription factor MEF/ELF4 regulates the quiescence of primitive hematopoietic cells. *Cancer Cell* **9,** 175–187
8. Liu, Y., Elf, S. E., Miyata, Y., Sashida, G., Liu, Y., Huang, G., Di Giandomenico, S., Lee, J. M., Deblasio, A., Menendez, S., Antipin, J., Reva, B., Koff, A., and Nimer, S. D. (2009) p53 regulates hematopoietic stem cell quiescence. *Cell Stem Cell.* **4,** 37–48
9. Fukushima, T., Miyazaki, Y., Tsushima, H., Tsutsumi, C., Taguchi, J., Yoshida, S., Kuriyama, K., Scadden, D., Nimer, S., and Tomonaga, M. (2003) The level of MEF but not ELF-1 correlates with FAB subtype of acute myeloid leukemia and is low in good prognosis cases. *Leuk. Res.* **27,** 387–392
10. Yao, J. J., Liu, Y., Lacorazza, H. D., Soslow, R. A., Scandura, J. M., Nimer, S. D., and Hedvat, C. V. (2007) Tumor promoting properties of the ETS protein MEF in ovarian cancer. *Oncogene* **26,** 4032–4037
11. Totoki, Y., Tatsuno, K., Yamamoto, S., Arai, Y., Hosoda, F., Ishikawa, S., Tsutsumi, S., Sonoda, K., Totsuka, H., Shirakihara, T., Sakamoto, H., Wang, L., Ojima, H., Shimada, K., Kosuge, T., Okusaka, T., Kato, K., Kusuda, J., Yoshida, T., Aburatani, H., and Shibata, T. (2011) High-resolution characterization of hepatocellular carcinoma genome. *Nat. Genet.* **43,** 464–469
12. Du, Y., Spence, S. E., Jenkins, N. A., and Copeland, N. G. (2005) Cooperating cancer-gene identification through oncogenic-retrovirus-induced insertional mutagenesis. *Blood* **106,** 2498–2505
13. Sashida, G., Liu, Y., Elf, S., Miyata, Y., Ohyashiki, K., Izumi, M., Menendez, S., and Nimer, S. D. (2009) ELF4/MEF activates MDM2 expression and blocks oncogene-induced p16 activation to promote transformation. *Mol. Cell Biol.* **29,** 3687–3699
14. Borer, R. A., Lehner, C. F., Eppenberger, H. M., and Nigg, E. A. (1989) Major nucleolar proteins shuttle between nucleus and cytoplasm. *Cell* **56,** 379–390
15. Falini, B., Mecucci, C., Tiacci, E., Alcalay, M., Rosati, R., Pasqualucci, L., La Starza, R., Diverio, D., Colombo, E., Santucci, A., Bigerna, B., Pacini, R., Pucciarini, A., Liso, A., Vignetti, M., Fazi, P., Meani, N., Pettirossi, V., Saglio, G., Mandelli, F., Lo-Coco, F., Pelicci, P. G., Martelli, M. F., and GIMEMA Acute Leukemia Working Party (2005) Cytoplasmic nucleophosmin in acute myelogenous leukemia with normal karyotype. *N. Engl. J. Med.* **352,** 254–266
16. Yu, Y., Maggi, L. B., Jr., Brady, S. N., Apicelli, A. J., Dai, M. S., Lu, H., and Weber, J. D. (2006) Nucleophosmin is essential for ribosomal protein L5 nuclear export. *Mol. Cell Biol.* **26,** 3798–3809
17. Mariano, A. R., Colombo, E., Luzi, L., Martinelli, P., Volorio, S., Bernard, L., Meani, N., Bergomas, R., Alcalay, M., and Pelicci, P. G. (2006) Cytoplasmic localization of NPM in myeloid leukemias is dictated by gain-of-function mutations that create a functional nuclear export signal. *Oncogene* **25,** 4376–4380
18. Falini, B., Bolli, N., Shan, J., Martelli, M. P., Liso, A., Pucciarini, A., Bigerna, B., Pasqualucci, L., Mannucci, R., Rosati, R., Gorello, P., Diverio, D., Roti, G., Tiacci, E., Cazzaniga, G., Biondi, A., Schnittger, S., Haferlach, T., Hiddemann, W., Martelli, M. F., Gu, W., Mecucci, C., and Nicoletti, I. (2006) Both carboxyl-terminus NES motif and mutated tryptophan(s) are crucial for aberrant nuclear export of nucleophosmin leukemic mutants in NPMc+ AML. *Blood* **107,** 4514–4523
19. Grisendi, S., Bernardi, R., Rossi, M., Cheng, K., Khandker, L., Manovae, K., and Pandolfi, P. P. (2005) Role of nucleophosmin in embryonic development and tumorigenesis. *Nature* **437,** 147–153
20. Rigaut, G., Shevchenko, A., Rutz, B., Wilm, M., Mann, M., and Séraphin, B. (1999) A generic protein purification method for protein complex characterization and proteome exploration. *Nat. Biotechnol.* **17,** 1030–1032
21. Suzuki, T., Kiyoi, H., Ozeki, K., Tomita, A., Yamaji, S., Suzuki, R., Kodera, Y., Miyawaki, S., Asou, N., Kuriyama, K., Yagasaki, F., Shimazaki, C., Akiyama, H., Nishimura, M., Motoji, T., Shinagawa, K., Takeshita, A., Ueda, R., Kinoshita, T., Emi, N., and Naoe, T. (2005) Clinical characteristics and prognostic implications of NPM1 mutations in acute myeloid leukemia. *Blood* **106,** 2854–2861
22. Colombo, E., Marine, J. C., Danovi, D., Falini, B., and Pelicci, P. G. (2002) Nucleophosmin regulates the stability and transcriptional activity of p53. *Nat. Cell Biol.* **4,** 529–533
23. Phelps, M., Darley, M., Primrose, J. N., and Blaydes, J. P. (2003) p53-independent activation of the hdm-P2 promoter through multiple transcription factor response elements results in elevated hdm2 expression in estrogen receptor α-positive breast cancer cells. *Cancer Res.* **63,** 2616–2623
24. Grisendi, S., Mecucci, C., Falini, B., and Pandolfi, P. P. (2006) Nucleophosmin and cancer. *Nat. Rev. Cancer* **6,** 493–505
25. Li, J., Zhang, X., Sejas, D. P., and Pang, Q. (2005) Negative regulation of p53 by nucleophosmin antagonizes stress-induced apoptosis in human normal and malignant hematopoietic cells. *Leuk. Res.* **29,** 1415–1423
26. Kondo, T., Minamino, N., Nagamura-Inoue, T., Matsumoto, M., Taniguchi, T., and Tanaka, N. (1997) Identification and characterization of nucleophosmin/B23/numatrin which binds the anti-oncogenic transcription factor IRF-1 and manifests oncogenic activity. *Oncogene* **15,** 1275–1281
27. Li, Z., Boone, D., and Hann, S. R. (2008) Nucleophosmin interacts directly with c-Myc and controls c-Myc-induced hyperproliferation and transformation. *Proc. Natl. Acad. Sci. U.S.A.* **105,** 18794–18799
28. Amati, B., Alevizopoulos, K., and Vlach, J. (1998) Myc and the cell cycle. *Front. Biosci.* **3,** d250–d268
29. Miyazaki, Y., Boccuni, P., Mao, S., Zhang, J., Erdjument-Bromage, H., Tempst, P., Kiyokawa, H., and Nimer, S. D. (2001) Cyclin A-dependent phosphorylation of the ETS-related protein, MEF, restricts its activity to the G_1 phase of the cell cycle. *J. Biol. Chem.* **276,** 40528–40536
30. Mao, S., Frank, R. C., Zhang, J., Miyazaki, Y., and Nimer, S. D. (1999) Functional and physical interactions between AML1 proteins and an ETS protein, MEF. Implications for the pathogenesis of t(8;21)-positive leukemias. *Mol. Cell Biol.* **19,** 3635–3644
31. Narayan, V., Halada, P., Hernychová, L., Chong, Y. P., Žáková, J., Hupp, T. R., Vojtesek, B., and Ball, K. L. (2011) A multi-protein binding interface in an intrinsically disordered region of the tumor suppressor protein interferon regulatory factor-1. *J. Biol. Chem.* **286,** 14291–14303
32. Bolli, N., Payne, E. M., Grabher, C., Lee, J. S., Johnston, A. B., Falini, B., Kanki, J. P., and Look, A. T. (2010) Expression of the cytoplasmic NPM1 mutant (NPMc+) causes the expansion of hematopoietic cells in zebrafish. *Blood* **115,** 3329–3340
33. Cheng, K., Sportoletti, P., Ito, K., Clohessy, J. G., Teruya-Feldstein, J., Kutok, J. L., Pandolfi, P. P. (2010) The cytoplasmic NPM mutant induces myeloproliferation in a transgenic mouse model. *Blood* **115,** 3341–3345
34. Vassiliou, G. S., Cooper, J. L., Rad, R., Li, J., Rice, S., Uren, A., Rad, L., Ellis, P., Andrews, R., Banerjee, R., Grove, C., Wang, W., Liu, P., Wright, P.,